

**T.C.
ISTANBUL GEDİK UNIVERSITY
INSTITUTE OF GRADUATE STUDIES**



**CENTRIFUGE MODELLING AND NUMERICAL ANALYSIS OF
HELICAL PILE IN EXPANSIVE SOIL**

MASTER THESIS

Raneen Ali Jasim AL-LAMI

**Civil Engineering Department
Civil Engineering Master in English Program**

**EYLÜL 2025
ISTANBUL**

**T.C.
ISTANBUL GEDİK UNIVERSITY
INSTITUTE OF GRADUATE STUDIES**



**CENTRIFUGE MODELLING AND NUMERICAL ANALYSIS OF
HELICAL PILE IN EXPANSIVE SOIL**

MASTER THESIS

**Raneen Ali Jasim AL-LAMI
(221291003)**

Civil Engineering Department

Civil Engineering Master in English Program

Thesis Advisor: Assoc. Prof. Dr. Redvan GHASEMLOUNIA

Istanbul 2025



T.C.
İSTANBUL GEDİK ÜNİVERSİTESİ
Lisansüstü Eğitim Enstitüsü Müdürlüğü

Jüri Tez Onay Formu

30/9/2025

LİSANSÜSTÜ EĞİTİM ENSTİTÜSÜ MÜDÜRLÜĞÜ

Bu çalışma 30/9/2025 tarihinde aşağıdaki jüri tarafından İnşaat Mühendisliği Anabilim Dalı, İnşaat Mühendisliği (Tezli Yüksek Lisans) Programı Yüksek Lisans Tezi olarak Kabul edilmiştir.

TEZ JÜRİSİ

Doç Dr. Redvan GHASEMLOUNIA

Danışman

İstanbul Gedik Üniversitesi

Dr. Öğr. Üyesi Hasan Bozkurt

NAZİLLİ

Üye (İmza)

İstanbul Gedik Üniversitesi

Dr. Öğr. Üyesi Mert TOLON

Üye (İmza)

İstanbul Maltepe Üniversitesi

DECLARATION

I'm Raneen Ali Jasim AL-LAMI, declare that this thesis titled “Centrifuge Modelling and Numerical Analysis of Helical pile in Expansive Soil” is original work I completed this to receive my master's in Civil Engineer. I further declare that neither this thesis nor any part of it has ever been submitted to or presented for a research paper or other degree at any other university or institution. (30/9/2025)

Raneen Ali Jasim AL-LAMI



PREFACE

Praise be to Allah, by whose grace all good and beautiful things are accomplished, and by whose guidance I have completed this academic work. I want to express my sincere thanks and appreciation to my supervisor, Prof. Dr. Redvan GHASEMLOUNIA, for his academic guidance, patience, and cooperation in completing this thesis. I would also like to express my sincere gratitude to Istanbul Gedik University for the opportunity that it provided me with learning in an environment rich in academic inspiration and practical experience. I would also like to express my gratitude and appreciation to my dear parents, my father, who gave me wings to soar, and my mother, who supported me with her love and prayers. I would also like to thank my sisters, my sister's husband, my older brother, and my best friend for their constant encouragement. Finally, I would like to thank everyone who supported me throughout this journey with a kind word, advice, or prayer from afar.

September 2025

Raneen Ali Jasim AL-LAMI

TABLE OF CONTENT

	Page No.
PREFACE	iv
TABLE OF CONTENT	v
ABBREVIATIONS	viii
LIST OF TABLES	ix
LIST OF FIGURES	x
ABSTRACT	xii
ÖZET	xiii
1. INTRODUCTION	1
1.1 Introduction	1
1.2 History of Helical Piles	1
1.3 Benefits of Screw piles.....	2
1.4 Applications for Screw Piles	3
1.5 The goals of the review	4
1.6 Thesis Structure	5
1.7 Practical Applications	5
2. REVIEW OF THE LITERATURE	6
2.1 Introduction	6
2.2 Screw Pile Installation.....	7
2.3 Impact of Installation	9
2.3.1 Installation effects on screw piles with solitary helix at expansive soils	9
2.3.2 Installation effects on screw piles with multi helix in expansive soil	10
2.4 Screw Pile Failure Mechanism.....	11
2.5 Geometric Factors in Screw Pile Design.....	11
2.5.1 Diameter of pile shaft	12
2.5.2 Spacing ratio impact (S/D_h).....	12
2.5.3 The number of helices (plates)	13
2.5.4 Helical fixation angle and pitch distance.....	14
2.5.5 The embedded depth ratio's effects	14

2.5.6 Effect of the D/d wing ratio	16
2.6 Screw Pile Capacity Estimation	16
2.6.1 Direct design methods	16
2.6.2 The theoretical design methods	19
2.6.2.1 Cylinder shearing technique	19
2.6.2.2 Method of individual bearing	23
2.6.3 Empirical approaches to design	25
2.7 Installation Torque Limitations	27
2.8 Prediction Load Settlement Curve of Ultimate Capacity	28
2.9 Previous Studies of Centrifuge and Small-Scale Anchor Models in Expansive Soil	31
3. THE PROCESS OF CENTRIFUGAL MODELING AND TESTING.....	33
3.1 Introduction	33
3.2 The Centrifuge Modeling Concept.....	34
3.3 Parts and Equipment of Centrifuge Devices	36
3.3.1 The control board.....	36
3.3.2 The arm and rotation axis	37
3.3.3 The system's main gearbox.....	38
3.3.4 Soil container	39
3.3.5 Screw pile installation	39
3.3.6 The results obtaining and monitoring.....	42
3.4 Measuring Settlement.....	43
3.5 Models of Screw Pile	43
3.6 Procedure of Testing	44
3.7 Testing Program for Foundations in Expansive Soil	47
3.8 The Scale Effect of Expansive Soil on Foundation Models.....	49
3.9 3 D Plaxis Software Program	50
4. METHODOLOGY.....	51
4.1 General	51
4.2 The effect of Materials on the Experimental Results	51
4.3 Numerical Modeling	51
4.4 The Effect of the Screw Pile Model's Spacing Ratio S/D	53
4.4.1 Impact of S/D ratio on bearing capacity	54
4.4.2 Comparative trends.....	55

4.5 Percentage Change in Bearing Capacity by S/D Ratio	60
4.6 Effect of Pitch Distance Screw Pile Model	61
4.7 Effect of S/D Ratio on Load-Settlement	63
4.7.1 Increase in diameter leads to improved load capacity	67
4.7.2 Effect of S/D ratio on load-settlement	67
4.7.3 Load-settlement behavior for different diameters	68
4.8 Comparison of Results with Previous Studies	68
5. CONCLUSIONS AND RECOMMENDATIONS	69
5.1 Summary	69
5.2 Conclusions	69
5.3 Recommendations	70
5.4 Limitations and Suggestions for Future Research.....	71
5.5 Contribution to Knowledge	71
REFERENCES	72

ABBREVIATIONS

AC Drive	: Alternating Current Drive
ASTM	: American Society for Testing and Materials
CFEM	: Canadian Foundation Engineering Manual
CPT	: Cone Penetration Test
D	: Diameter of Helix
D	: Diameter of Shaft
E	: Young's Modulus
g	: Gravitational Acceleration
H	: Embedment Depth
K₀	: Coefficient of Earth Pressure at Rest
K_s	: Coefficient of Lateral Earth Pressure (Compression)
K_u	: Coefficient of Lateral Earth Pressure (Uplift)
kN	: Kilo Newton
LCPC	: Central des Ponts et Chaussées
N	: Scaling Factor (Centrifuge)
N_q	: Bearing Capacity Factor
PLAXIS	: Finite Element Software for Geotechnical Analysis
R	: Radius
RPM	: Revolutions Per Minute
S/D	: Spacing Ratio (Distance Between Helices / Helix Diameter)
SSI	: Soil-Structure Interaction
T	: Torque
γ	: Unit Weight of Soil
φ	: Angle of Internal Friction
ω	: Angular Velocity

LIST OF TABLES

	Page No.
Table 2.1: Critical Embedment Ratio, $(H/D)_{cr}$, is Presented in as Determined by ...	22
Table 2.2: The uplift coefficients, K_u , for helical anchors, are shown in .	23
Table 2.3: The Bearing Capacity Factor, N_q , for Cohesion Less Soils	24
Table 2.4: The Typical Values of K_o for Normally Consolidated Expansive Soil	25
Table 3.1: The Prototype and Model's Scale Factor	36
Table 3.2: The Main Gearbox Properties	38
Table 3.3: The Torque and Rotational Speed for Some Helical Piles Installation	40
Table 3.4: The First and Gearbox Details, Respectively	41
Table 4.1: The Soil Parameters for Expansive Soil and Sand (Undrained Behavior)	53
Table 4.2: The Screw Pile Model's Bearing Capacity with Different S/D Spacing Ratios	54
Table 4.3: From the Inputs and Results for Diameter = 0.4m:	56
Table 4.4: From the Inputs and Results for Diameter = 0.5m	57
Table 4.5: From the Inputs and Results for Diameter = 0.6m	58
Table 4.6: The Percentage Increase in Bearing Capacity	61
Table 4.7: The Pitch Distances (m) for Different Helix and Diameters	61
Table 4.8: Load-Settlement Values for Different S/D Ratios and Helix Numbers when Diameter (0.3m)	64
Table 4.9: Load-Settlement Values for Different S/D Ratios and Helix Numbers When Diameter (0.4m)	65
Table 4.10: Load-Settlement Values for Different S/D Ratios and Helix Numbers when Diameter (0.5m)	66
Table 4.11: Load-Settlement Values for Different S/D Ratios and Helix Numbers When Diameter (0.6m)	67

LIST OF FIGURES

	Page No.
Figure 1.1: A Screw Pile Geometry	2
Figure 1.2: Screw Pile Application Locations	4
Figure 2.1: A Typical Screw Pile Layout	7
Figure 2.2: Helical Pile Placement Field Apparatus	8
Figure 2.3: Individual Helix Approach (a) and Cylindrical Shear Method (b) as Theories of Failure Mechanisms	12
Figure 2.4: Screw Pile with A Shaft-Helix Arrangement	14
Figure 2.5: (a) The Relationship between Uplift Resistance and Soil Depth; (b) The Relationship between Wing Stress and Wing Ratio	16
Figure 2.6: Procedure for Determining Equivalent Cone Impedance Using the LCPC process	18
Figure 2.7: The Details of Cylindrical Shear Failure under Tension and Compression Loading	20
Figure 2.8: The Breakout Factor Variation for (a) Shallow Screw Piles and (b) Deep Screw Piles with Respect to Soil Friction Angle and the H_{ht}/D Ratio....	22
Figure 2.9: The Distribution of Force in the Singular Bearing Method for Screw Piles under Compressive Load Is Presented By	25
Figure 2.10: Typical Load-Displacement Curves	28
Figure 2.11: Curve Regions of Load Displacement	29
Figure 3.1: Describe How the Prototype and Model's Vertical Stress Distributions.	35
Figure 3.2: The Model and Prototype Are Compared In Terms Of How Stress Changes with Depth	36
Figure 3.3: Control Board Detail	37
Figure 3.4: The Centrifuge Arm and Rotation Axis	38
Figure 3.5: The Centrifuge System Main Gearbox	38
Figure 3.6: The Soil Container	39
Figure 3.7: The Relationship between Torque Speed and Rotation Rate	41
Figure 3.8: First Gearbox	41

Figure 3.9: Described the Horizontal Shaft's Movement inside the Quid Steel	42
Figure 3.10: The Cell Load	42
Figure 3.11: The Indicator Digital	43
Figure 3.12: The Two Dial Gauges.....	43
Figure 3.13: The Screw Pile Models' Dimensions and Configurations In.....	44
Figure 3.14: Second Gearbox and the Fixating Screw Pile	45
Figure 3.15: The Installation Screw Piles	46
Figure 3.16: The Painting of the Soil-Covered Plate	46
Figure 3.17: The System Centrifuge	47
Figure 3.18: An Inclined Load	48
Figure 3.19: A Vertical Load	49
Figure 3.20: Project Properties Window in PLAXIS 3D.....	50
Figure 4.1: Expansive Soil Layer Overlying Sand Layer in a Soil Profile	52
Figure 4.2: The Ultimate Bearing Capacities for Screw Piles with one Helix and Two Helices When Helix Diameter (0.3m).....	54
Figure 4.3: The Ultimate Bearing Capacities for Screw Piles with One Helix and Two Helices When Helix diameter (0.4 m)	55
Figure 4.4: The Ultimate Bearing Capacities for Screw Piles with One Helix and Two Helices When Helix Diameter (0.5 m)	57
Figure 4.5: The Ultimate Bearing Capacities for Screw Piles with One Helix and Two Helices When Helix Diameter (0.6 m)	58
Figure 4.6: The Updated Bearing Capacity Results for Helix Diameters of 0.3 m, 0.4 m, 0.5 m, and 0.6 m with Different S/D Ratios	59
Figure 4.7: Percentage Increase in Bearing Capacity (%) Relative to S/D Ratio	60
Figure 4.8: Pitch Distance vs. S/D Ratio for Single and Double Helix Screws.....	61
Figure 4.9: Load Settlement Curves for Helical Piles When Diameter (0.3m)	63
Figure 4.10: Load Settlement Curves for Helical Piles When Diameter (0.4m)	64
Figure 4.11: Load Settlement Curves for Helical Piles When Diameter (0.5m)	65
Figure 4.12: Load Settlement Curves for Helical Piles When Diameter (0.6m)	66

CENTRIFUGE MODELLING AND NUMERICAL ANALYSIS OF HELICAL PILE IN EXPANSIVE SOIL

ABSTRACT

The performance study of helical piles embedded in expansive soils, conducted with the help of numerical analysis and centrifuge modeling, is presented in this dissertation. Any foundation system is significantly hampered by expansive soils, which are generally recognized for their high swell-shrink characteristics brought on by changes in moisture content. Because of the unique geometry and installation method using helical piles, stability and load-bearing capacity improvement options may be offered to guarantee adequate performance under such problematic soil conditions.

For the purpose of establishing field stress conditions and altering key geometric parameters the helix pitch distance, number of helices, spacing ratio S/D , and helix diameter and their effects on the axial uplift and compression capacity of screw piles, the study employs physical modeling using a centrifuge. In order to evaluate behavior under non-vertical forces, conditions were inclined piling forces operated were also modeled. To investigate scale effects and uplift failure mechanisms, these small-scale models were tested at various g levels.

To validate the experimental results, learn about failure modes, and improve the design, numerical analysis was done using previously developed theories, such as individual bearing and cylindrical shear. The results demonstrated that load resistance under uplift is greatly increased by increasing the number of helices and optimizing their spacing. These parameters were important in the optimization of screw pile performance under various loading conditions as the results indicated. In addition, the centrifuge tests' results were in line with theoretical forecasts, so modeling that specific strategy can be considered reliable.

The behavior of screw piles in expansive soils is examined holistically in this study, which also provides engineers with a useful manual on how to design a solid foundation for buildings in swell-prone areas.

The dynamic effects were not taken into account in this research. The primary purpose of the study was to test the behavior of helical piles under controlled load conditions in expansive soil in terms of its load bearing behavior in the statical position. Dynamic or cyclic loading adds other parameters of damping ratio, frequency response, inertia effects, and other special instrumentation and boundary conditions are needed. Because the present work was aimed at the verification of the static uplift and compressing capabilities, the dynamic effects would have complicated the interpretation of the model and would not have been in line with the main research goals. Consequently, dynamic behavior was not included and only quasi-static load applications were taken into consideration, so that clarity and accuracy of the evaluation of the pile soils interaction would be achieved. That will be addressed in future research. Dynamic effects will be addressed in future research.

Keywords: *Helical piles, Expansive soils, Centrifuge modeling, Numerical analysis, Bearing capacity.*

ŞİŞEN TOPRAKTA SARMAL KAZIĞIN SANTRİFÜJ MODELLEMESİ VE SAYISAL ANALİZİ

ÖZET

Bu tez, santrifüj modelleme ve sayısal analiz yardımıyla genişleyen zeminlere gömülen helisel kazıkların performans çalışmasını sunmaktadır. Genleşen zeminler, genellikle nem içeriğindeki değişikliklerden kaynaklanan yüksek şişme-büzülme özellikleriyle bilinir; bu nedenle, herhangi bir temel sisteminde önemli sorunlar yaratırlar. Helisel kazıkların özel geometrisi ve montaj tekniği sayesinde, sağlanabilecek stabilite ve yük taşıma kapasitesi iyileştirme alternatifleri, bu tür sorunlu zemin koşullarında yeterli performansı garanti eder. Çalışmada, saha gerilim koşullarını uygulamak ve helisel adım mesafesi, helisel sayısı, aralık oranı S/D ve helisel çapı gibi temel geometrik parametreleri, vidalı kazıkların eksenel kaldırma ve basınç kapasitesi üzerindeki etkilerini değiştirmek için bir santrifüj aracılığıyla fiziksel modelleme kullanılmıştır. Ayrıca, eğimli kazık kuvvetlerinin etki ettiği koşullar modellenerek, düşey olmayan kuvvetler altındaki davranış değerlendirilebilmiştir. Bu küçük ölçekli modeller, ölçek etkilerini ve kaldırma hasarının mekanizmalarını incelemek için farklı g seviyelerinde testlere tabi tutulmuştur. Silindirik kesme ve tekil yataklama gibi halihazırda geliştirilmiş teorilerin yardımıyla sayısal analiz, deneysel sonuçların geçerliliğini kontrol etmek ve hasar modları ve tasarım optimizasyonu hakkında bilgi edinmek için gerçekleştirilmiştir. Sonuçlar, helis sayısının artırılmasının ve aralıklarının optimize edilmesinin, kaldırma kuvveti altındaki yük direncini önemli ölçüde artırdığını kanıtlamıştır. Bunun yanı sıra, santrifüj testlerinden elde edilen çıktı teorik tahminlerle tutarlıydı; dolayısıyla, bu özel yaklaşımın modellenmesi güvenilir kabul edilebilir.

Bu çalışma, vidalı kazıkların genişleyen zeminlerdeki davranışına bütünsel bir bakış açısı sunmakta ve mühendislere, şişmeye eğilimli ortamlarda yapılar için etkili bir temel oluşturma konusunda pratik bir rehber sunmaktadır. Genleşen zemindeki helezon kazıkların yük taşıma davranışının hareketsiz hâlindeki etkisine odaklanmak için dinamik etkiler ortadan kaldırıldı. Bunların dahil edilmesi gereksiz bir karmaşıklığa yol açacaktı. Sadece yarı statik yükleme analiz edildi ve gelecekteki çalışmalarda dinamik etkiler önerildi.

Anahtar Kelimeler: *Helisel kazıklar, Genleşen zeminler, Santrifüj modelleme, Sayısal analiz, Taşıma kapasitesi.*

1. INTRODUCTION

1.1 Introduction

A helical pile is a hollow steel tube with a round shape constructed from steel with one or multiple steel spirals welded to the hollow tube. Every metal spiral is welded at a 90-degree angle to the metal rod. The helical pile has a groove with a 45° slope in the end tube (shaft) to ease the soil's placement processes (penetration). Figure (1.1) describes the shape of the screw pile. Several of the coil (individual, paired, and triple coil) that should be utilized in the screw anchor depending on the anchor capacity and soil conditions and the distance between two coils significantly impacts the capacity of the screw anchor. The screw pile's core shaft is utilized to transfer axial loads (tension and compression load) to the spiral. Additionally, to transfer rotational force while driving the screw pile into the soil. The main column also withstands sideways forces. Helical piles have strong compression and tension capability and can be utilized for various ground conditions below and above water. In addition, the helical pile offers a cost-effective and rapid installation when compared to other types of piles. Screw pile foundations are also known as torque piles, helical anchors, screw anchors, posts, or helical piles [41].

1.2 History of Helical Piles

Screw piles were utilized as bases for bridges and structures constructed on soggy or unstable soil. They had restricted use in the 19th and early 20th century, where the installation of a screw pile was challenging without mechanical technology. During the 1960s, the technology of helical pile manufacturing and installation was developed. Therefore, helical piles are crucial for designers and engineers because of their strong resistance to both tension and compression forces. Because of this advancement in technology, the utilization of a screw pile had significantly expanded.

Throughout the globe, particularly as hydraulic torque motors became accessible and the mounting technique of screw pile became significantly easier. Screw piles were initially used mainly for withstanding pulling forces. Utility companies often use helical piles as anchoring hardware for transmission towers and utility poles. Last year saw helical piles being used in many engineering applications. The stacks' robust resilience to both carrying and upward pressure allows them to be used in situations where resistance to combinations of pulling and pushing forces are needed.



Figure 1.1: A Screw Pile Geometry

1.3 Benefits of Screw piles

Helical also called screw piles or helical piles or helical anchors consist of deep foundation components comprising of steel shafts with one or multiple helical plates welded at the tip. Installation is done by spinning them into the ground with hydraulic equipment as though it were a huge screw. This technique reduces the disturbance of the soil, is easily installed, excavation and concrete curing are not required, and the construction has immediate bearing capacity. Screw piles have been

extensively applied in supporting buildings, bridges, transmission towers and other constructions in a vast variety of soil types especially where there is limited access or where rapid construction is necessary.

1. Shorter set-up and establishment times that need less work than other heap choices, for certain specific machines just requiring one affirmed installer.
2. Easy to expand and join in-situ.
3. Simple to eliminate whenever expected for a transitory circumstance with no harm to the screw heap, empowering re-use.
4. Possible to introduce in regions with unfortunate availability, for instance, where there is low headroom or different kinds of restricted spaces.
5. Can be introduced at a tendency, basically for mooring inclines
6. Minimal vibration and development commotion during establishment contrasted with other heap techniques are fundamental while introducing establishments close to vibration and clamor delicate designs or underground administrations.
7. Can be introduced in practically any climatic condition (just the most outrageous ground temperatures or air weather patterns will influence appropriate establishment).
8. Reduced removal costs, for the most part where the ground is sullied, because of very little ruin made by the helix during establishment.
9. Can be stacked (counting for load testing) following establishment (except if substantial setting time is expected subsequent to infilling).
10. Installation force gives a sign of ground strength at each heap. Impermanent backings, like housings, are not needed in delicate or unsteady ground.

1.4 Applications for Screw Piles

The following are applications for screw piles in construction and performance:

New establishments	Mooring
<ul style="list-style-type: none"> • Transmission towers and seaward and inland wind turbines. • Modern, business and private structures. • Movable structures scaffolds, breakwaters, and wharves. • Scaffolds, breakwaters, and wharves. • Gantries for signals. • Pipes. 	<ul style="list-style-type: none"> • Extremely strong support for existing or new bridges and retaining structures. • Temporarily fastening equipment, especially to prevent lifting. Piles are removable and reusable. • Slant adjustment and slip remediation, especially in the event that it is called for in a brief period of time.

Figure 1.2: Screw Pile Application Locations

1.5 The goals of the review

The goals of this study are:

1. Utilizing centrifuge modeling, examine how the screw pile prototype behaves. This includes: -
 - a. The impact of the pitch distance of the helix on the compression and uplift capacities.
 - b. The impact of the spacing proportion s/d (spacing between helices) on the capacity for uplift and compression.
 - c. The impact of the helix's width on the capacity for uplift and compression.
 - d. The impact of the quantity of helices on the capacity for uplift and compression.
 - e. The screw heap's elevate limit under slanted inspire load with an alternate point with the skyline.
 - f. The uplift capability of the screw pile under an angled uplift load at an oblique angle to the horizon.
2. Examining how the screw pile behaves at various centrifuge force settings.
3. Assess the theoretical methods for estimating screw piles' maximum capacity.

1.6 Thesis Structure

Chapter one, the screw pile has a prologue which includes the history of the screw pile, the benefits and use of screw piles, and the purpose of the review.

Chapter two presents many theoretical and empirical equations to compute the bearing and uplift capacity, prediction of the value of torque, and a literature review of the past research on screw piles.

Chapter three describes the principle underlying the centrifuge, how the centrifuge system is designed and manufactured, the characteristics of the soil used in the models, the method, and the testing program in detail.

Chapter four reports and analyzes the findings, which reveal all the findings of the relationship between tension and compression load and settlement of the different screw pile model setups under small-scale and centrifuge modeling, and also the discussion of the reason why the bearing and uplift ratio is improved.

Chapter five offers conclusions and recommendations that summarize the main findings of the research and give recommendations to conduct further research on the subject matter.

1.7 Practical Applications

The information derived out of the study can be used in:

- The engineering design of foundations of infrastructure works in expansive soils [17,41].
- Formulation of direction to geotechnical engineers in order to maximize screw pile configurations [7,8,41].
- Improving the predictively of numerical modeling in the prediction of screw pile behavior [21,24].

This study has contributed to the wider aspect of geotechnical engineering by addressing these aspects which forms a basis to develop future studies of deep foundation systems [9,19,47].

2. REVIEW OF THE LITERATURE

2.1 Introduction

Albeit regular piles as a profound starting point for seaward and coastal undertakings are deeply grounded innovation (i.e., driven, bored, or in situ and mono piles), there is a need to build the pile limit by diminishing the number of piles and diminishing in the expense of any venture. Screw pile opposition might arrive at up to 2-3 of the pile's ability. The establishments address approximately 30% roughly for the absolute expense of these foundation projects, particularly for enormous undertakings (i.e., multi-story buildings, storehouses, electrical power plants, and wastewater treatment plants) or seaward activities of trouble the establishment interaction. Consequently, the helical piles are created before the exploration in geotechnical design to examine the obstruction for elevate and pressure powers and how they act under the pivotally applied loads from the actual construction. The helical pile has a right bearing and tension capacity and is used for different soils under and over water. The other advantage is that the helical pile has quicker installation than conventionally driven piles. Screw piles are reasonable to oppose for both pressure loads (for example, wastewater treatment plants, multi-story buildings, and docks under the scaffold) and strain loads (for example, a storehouse, the groundwork of the breeze energy turbine, the groundwork of electrical energy transmission pinnacles, and correspondence towers). The setup of screw piles is intended to give adequate stacking limit through a solid, low-unsettling influence and quick establishment technique. One or more helix plates that have been soldered to a central shaft make up a screw pile. The diameter D , number, pitch distance, ratio of spacing (S / D), and ratio of depth embedment to a diameter (H / D) of the upper helix are totality factors in the construction and analysis of a pile with helices. The shaft length pile and pile diameter are also chosen. The screw pile's maximum capacity for compression and uplift can be effects of by all of the recently referenced factors. screw pile's maximum capacity for compression and uplift can be influenced by all of the previously mentioned factors. In addition to choosing the best approach,

specific performance and loading requirements are taken into account while designing screw piles. The center steel shaft is shaped as an empty round pipe or a strong bar square. Diameter and pitch spacing of the helix plates can be adjusted to provide the required bearing force for the installation of the specified soil embedment. To ensure that reduce the amount of soil unsettling influence and facilitate the torque process during screw pile installation, the helix and pitch diameter were chosen. Conventional foundation analysis techniques like Terzaghi's generic formula for bearing capacity (Terzaghi, 1943) [50] have influenced the development of screw pile design. Appropriate adjustments were included to accommodate the thin geometry of pile construction and the individual helical plate components. As a result of these adjustments, two analysis and design techniques have been developed: A shear in a cylinder resistance technique and an individual helix-bearing approach. Every technique has its own approximations and analytical definition. The main configurations of a helical pile are shown in Figure 2.1.

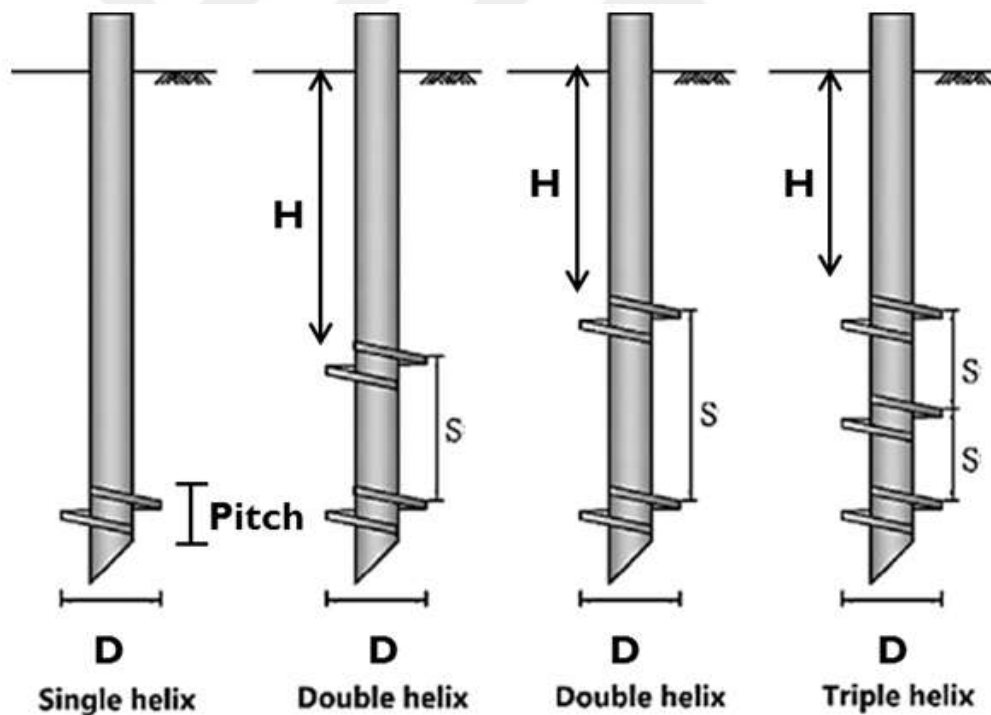


Figure 2.1: A Typical Screw Pile Layout [56]

2.2 Screw Pile Installation

One of the main benefits of the helical pile is its easy, affordable, and ecologically friendly installation method. This is one of the reasons screw piles are becoming more and more popular in a variety of industries (offshore and onshore

projects). According to AL Baghdadi et al. (2017), the traditional pile construction method involves using heavy weights at a specific height of drop and impacting the pile with a pile driver. This causes noise and vibration that is harmful to the surrounding area, the environment, and the building that is close by. Thus, in order to install screw piles into the ground, a vertical downward pressure known as crowd load is provided. This makes the installation process easier and makes use of the torque that the engine applies to the machine in order to support the hydraulic equipment [61]. While some screw piles may be able to reach the necessary depths because to the higher vertical crowd load, some piles are not able to surpass their torque capacity [54]. According to Perko (2009) [41], the optimal pace at which a screw pile penetrates the ground should be one pitch distance each rotation. Perko (2009) suggested that the motor used for the installation of screw piles should have a low rotation speed and high torque to minimize soil disturbance. This would prevent the soil from being sheared during the process and result in significantly less environmental disturbance (noise and vibration) with a shorter installation duration. The state of the area where the helical piles are installed determines the choice of installation equipment. During installation, a driving motor-head, a rotary motor driven by hydraulic energy that is installed on a boom truck or skid steer excavator provides the applied torque. It is stickled to the screw pile head [15]. The helical pile's installation field equipment is detailed in figure 2.2.



Figure 2.2: Helical Pile Placement Field Apparatus [45]

2.3 Impact of Installation

The ultimate bearing capacity for uplift and compression is greatly impacted by the positioning of the screw pile because it changes the soil where the displaced and sheared plates move laterally and vertically.

2.3.1 Installation effects on screw piles with solitary helix at expansive soils

In case of pile screw with single helix and expanding soil, there are factors such as construction workmanship that ought to be considered as they will determine the performance of the screw pile especially the uplift capacity. Expansive soils develop the unique feature of changing their volumes to a great extent depending on the amount of moisture present unlike conditions in clay or sand types of soils.

Have studied some installation effects of a pile of screw with single helix into the expansive soils [31]. They note that the movement of soil particles around the helix during the installation is more complicated due to the presence of expansive soil. The soil displacement and even the stresses around the helix are unlike those observed in lower compressive soils. The mentioned research pinpointed the reality that the soil particles surrounding centric helix aren't only backfilled appositely but undergo tremendous change in volume as a result of soil engulfing or disbanding. This changes the nature of the adjoining soil to the centric helix.

The experiments conducted by [43] involved embedding a model screw pile of one single helix type into expansive clay. The findings indicated that during placement, a downward mass flow of soil particles occurs below the level of the helix into the lower section whilst upward mass flow occurs above the helix where the soil is quite likely to be set loose due to swellings characteristic of expansive soils. The displacement was credited to the action of the screw pile, which also exerts a radial as well as an axial force upon the soil. The author of the article stated that besides the immediate disturbance of the helix above soil surface, long term soil swelling and shrinking effects also impact soil mass response above the helix.

Evaluated the influence of the installation along with a single inclining screw pile in expansive soils. It was shown that post construction behavior of the soil played a vital role in the screw pile's uplift capacity [21]. Within their study they

were able to prove these numerical simulations using finite element analysis: the uplift resistance was bound to be low as long as the blind soil problems over the helix were not resolved. These insights were confirmed by the experiments which showed that the soil thrust during installation deteriorated indeed the uplift capacity obtained in practice without any solid countermeasures. The explanation was mainly due to the fact that the expansive soil had already reacted to construction which is not accurately reflected in the numerical work.

2.3.2 Installation effects on screw piles with multi helix in expansive soil

The contact between the screw piles with multi-helix and the expansive soil during the construction of screw pile is impacted by the properties for expansive soils, which in this case are their swelling and shrinkage behaviors. When a multi-helix screw pile is driven, the helicoids blades first displace the expansive soil vertically and to the side. This type of interaction is by and large cylindrical shear (rubbing) like that of sand, but the 'sand', which is expansive clay, differs from that of the normal sand processes.

Worthy of noting, as [59] state, they experienced tremendous volume changes as the screw pile was torqued down. Some soil within the helix structures follows the screw-shaped vertical blade and is displaced both vertically and radically outwards. The expansive type of soil behaves distinctly from water-saturated sand because it can swell considerably, which retrogresses the helixes interaction. They may produce added loads as well as changes in the soil matrix during the installation or afterward.

Mono-well-constructed multi-helix screw piles in expansive soils lead to large shear strains and excess pore water pressure, [42] explained. It is also noted that installation of piles in expansive soil construction expert tips may adversely impact the soil in the early corrective action management, as this is attributed to moisture content increase and disturbance of soils. As the moisture content of the soil over time returns to its natural state, the properties of the cylindrical volumetric space situated over the helixes may differ from those prevailing at the time of installation.

These interactions also depend on factors such as the geometry of the helical pile's number of helixes and their installation in the expansive soil at different initial moisture contents. Since the helixes are cemented into the piles to a certain depth, the

vertical and lateral displacements resulting in the helices may displace the soil mass upwards and/or consolidate the material near the pile, resulting in modification of the soil mass overhead the top helix in comparison to that underneath bottom helix.

According to [14], extra helices did not increase extra capacity for the pile as the case with sand, but moisturized expansive soil determined the amount of extra helices. For extra helix, it can be explained that the more helices added, the more complicated the interaction becomes up to a limit where further inclusion of helices has little, if any, positive gain because of excess volumetric contraction or expansion of the soil. When it comes to helix and expansive soils, the individual soil properties encircling each helix less and more in most cases may be more than those exposed above and below the helix; therefore, the stability and | The pile's capacity to support a load may be affected differently.

2.4 Screw Pile Failure Mechanism

As was previously mentioned, in order to estimate the theoretical uplift and helix bearing capacity (screw) piles inside the context for traditional soil mechanics, the two main theories based on the mechanism of failure during loading must be taken into consideration: the solitary bearing helix theory as well as cylindrical shear resistance theory. Which the mechanism of failures, the solitary bearing failure theory or the shear of cylinder resistance failures theory, applies under loading relate to interactions between the soil-pile steel shaft and the soil-helix .This affects both the analysis and design. According to [30], the soil conditions, helical spacing, and pile embedment depth have an impact on the helical pile bearing capacity. [62] further divided helical piles into shallow and deep anchors, emphasizing important characteristics such as helices number, a helix diameter, an embedment depth of the screw pile, and spacing ratio (S / D), This is the diameter to any two plate's ratio. [61,44]. The failure processes of helical piles are depicted in Figure 2.3.

2.5 Geometric Factors in Screw Pile Design

Numerous geometrical characteristics influence a helical pile's both the analysis and the design. The ultimate capability and behavior screw piles are impacted by these characteristics in distinct ways. The diameter helix (D_h), pitch

distance of the helix, diameter of shaft (d), spacing ratio (S/D_h), quantity of helical plates, and embedment depth of the helical plates are some of these characteristics[15].

2.5.1 Diameter of pile shaft

The screw pile's ultimate bearing and uplift capacity will be significantly impacted by the shaft diameter. The shaft diameter impacts the adhesion or frictional resistance of the screw pile by increasing surface area. Furthermore, a bigger volume of displaced soil is produced by an increase in shaft diameter, and this leads to localized densification just around the installed screw pile. Research by Narasimha (1991) [34], which discovered that the overall surface area for shaft pile significantly impacts bearing capacity and ultimate uplift of screw piles, lends credence to this.

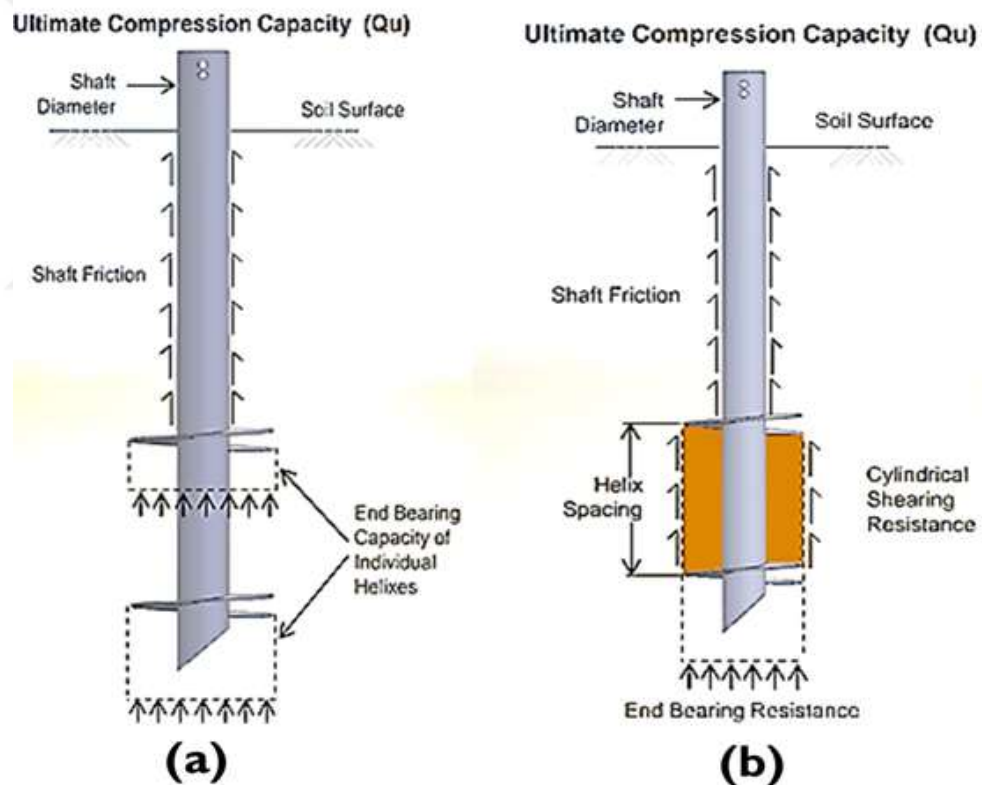


Figure 2.3: Individual Helix Approach (a) and Cylindrical Shear Method (b) as Theories of Failure Mechanisms [34]

2.5.2 Spacing ratio impact (S/D_h)

The impact of spacing ratio (S/D_h) on helical piles' capability in expansive soil has been explored through various studies. The impact of helix spacing (the distance between adjacent helices) on pile capacity under both compression and

tension loads in expansive soils was investigated [44]. In uplift capacity tests, significant interaction effects are caused by closely spaced helices, leading to the cylindrical shear surface theory being used for the bearing capacity computation. When the helix diameter is sufficiently large, interaction effects are reduced, allowing resistance to be developed by each helix based on the individual bearing theory. Typically, higher ultimate capacities under compressive loading are achieved with smaller spacing ratios (S/D_h). It was observed [34] that a spacing ratio (S/D_h) larger than 1.5 leads to a shift from single-bearing failure to cylindrical shear failure. Higher bearing capacities were demonstrated [62] in screw piles with a ratio of spacing ($S/D_h=1.5$) compared to those with a ratio of spacing ($S/D_h=3.0$) in expansive soils. The applicability of cylindrical shear failure was confirmed [49] for adjacent helices spaced at $1.5D_h$, with a spacing of $3D_h$ being typically required to observe a change in failure mechanisms. It was reported [27] that cylindrical shear failure governs screw pile behavior when the spacing ratio (S/D_h) exceeds 2.25, while individual bearing failure becomes dominant beyond this ratio. The association of a spacing ratio for single bearings larger than two failure was proposed [36] to achieve the most accurate ultimate bearing capacity in expansive soils.

2.5.3 The number of helices (plates)

A helical pile can be constructed with one or multiple helical flanges that are evenly spaced along the pile shaft. It is generally believed that both uplift and bearing capacity are enhanced by increasing the number of helices. For a single-helix screw pile, capacity is achieved through bearing on the plate area and the frictional resistance of the shaft. When the distance between two helices is reduced, a cylindrical shear soil mass is formed between them, resulting in an increased surface dimensions available in order to mobilize either incoherent (frictional) immovability in coarse-grained soils or cohesive resistance in fine-grained soils [15]. Additionally, weight of the soil inside this mass can be added to uplift immovability. Vertical capacity is generally enhanced by increasing the number of helices, whether under tension or compression forces. This behavior has been confirmed through experimental evidence, with an increase in capacity of more than 30% observed when screw pile configurations with two to four helices were compared, with all other factors remaining constant [33].

2.5.4 Helical fixation angle and pitch distance

In general, the proper helix shape is important to minimize soil disturbance when installing helix in soil. The shape of helix includes the angle at which the helix is fixed to the pitch distance at which the helix plate secures the helix and the helix pile shaft [15]. At a 90-degree fixing angle, the helix plate was welded to the helix., as shown in Figure 2.4. The distance along the helix pile shaft that separates the helix's top and bottom is known as the helix pitch. It was observed [13] that the helix pile fixing torque increases with the ratio of pitch distance to helix diameter (p/D) and helix angle ($\tan^{-1}(p/\pi D)$).

According to [58], as the size of a screw pile model increases, a decrease in cuticle friction is observed when a helical pile with a larger pitch distance is used. This reduction is attributed to increased ground resistance, which subsequently lowers both the bearing capacity and construction efficiency.



Figure 2.4: Screw Pile with A Shaft-Helix Arrangement

2.5.5 The embedded depth ratio's effects

Embedment ratio is defined as the ratio between depth (H) from the upper of helical to the surface soil over it and diameter (D) for upper helix [61]. Helical pile analysis and design are thought to heavily depend on this ratio (H/D). According to [28] theory, a shallow failure condition is associated with helical piles where $(H/D) < (H/D)_{cr}$ while a deep fail condition is exhibited through those where $(H/D) > (H/D)_{cr}$. Three classifications of embedment depth were established [33] in a test setting study

on small sized screw samples piles; $(H/D) < 2$ for shallow conditions; $2 < (H/D) < 4$ for transitive conditions; and $(H/D) > 4$ for deep conditions.

It was observed by [61] that in relation to the embedment ratio as the embedment ratio increases, Under tensile and compressive pressures, the screw pile's capacity increases in cohesive and cohesion-less soils, with a notable increase in uplift capacity under tensile loads. The critical influence of minimum embedment depth on screw pile performance was highlighted [41]. Shallow failure modes may be experienced in screw piles with insufficient embedment, particularly when The bearing helix plates are either in close proximity to an active soil wedge or the surface soil.

The significance of soil advantage in relation to individual bearing failure, cylindrical, and shear failure is reflected in the various equations used to calculate screw pile capacity, which account for different soil parameters. Parameters such as adhesion factors, angle of internal friction, unit weight for soil, untrained shear strength, bearing capacity parameters, and soil cohesion are primarily depended upon for the maximum amount that screw piles can hold.

It was noted [61] That in the soil with clay composition, a similarity in the bearing capacity in compression and tension is observed due to adhesion, while in cohesion-less soils, a slightly higher ultimate bearing capacity is noted due to end-bearing resistance. Variations in the features of the undisturbed the soil below helix and disturbed soil above it can result in differences in bearing capacities between compression and tension.

It was suggested [57] that solitary bearing method mainly focuses on each plate's bearing capacity, which reaches Relative to cylindrical shear modes, it peaks at higher settlement, where the peak value of the shear failure zone is attained at a lower settlement. It was further explained [45] that a higher ultimate capacity is exhibited by helical piles under compressive loads compared to those under tensile loads, the soil plug's area is included in the bottom helix's surface area when it is compressed, but only the top surface area of the helix is included when it is in tension.

2.5.6 Effect of the D/d wing ratio

The relationship between the wing diameter (helix) and shaft diameter (pipe) was examined [32]. In the study, a screw pile with a 40 mm shaft diameter was used to check the impact wing ratio on uplift capability, with wing ratios of 1.5, 1.75, 2.0, 2.5, and 3.0 (where the helix diameter ranged from 60 mm to 120 mm). It was found that uplift resistance of the screw piles increased as both the wing ratio (D/d) and pile depth increased (see Figure 2.5 A). Additionally, it was demonstrated that wing stress increased as the wing diameter ratio decreased (see Figure 2.5 B), highlighting the specific effect of wing stress on the wing ratio.

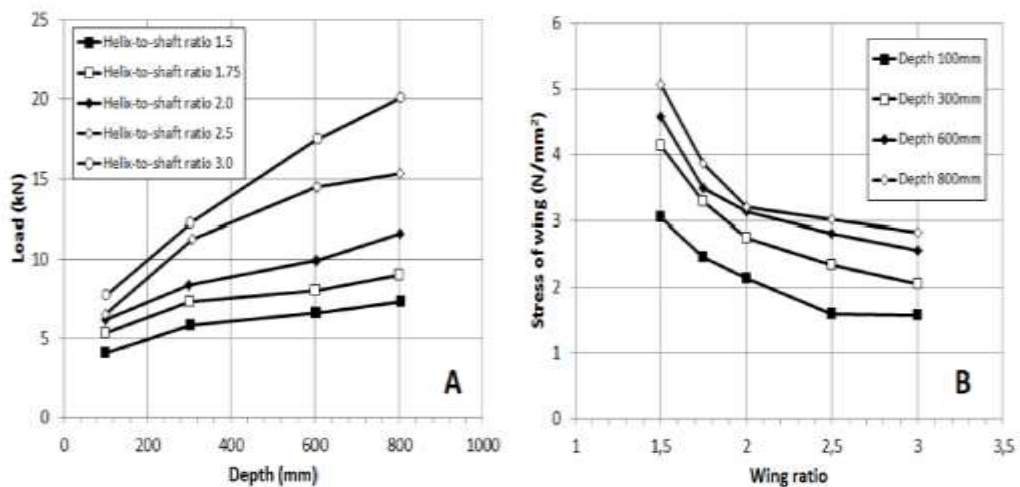


Figure 2.5: (a) The Relationship between Uplift Resistance and Soil Depth; (b) The Relationship between Wing Stress and Wing Ratio [32]

2.6 Screw Pile Capacity Estimation

In general, the methods used to predict the uplift and compression capability for screw piles implanted in cohesion less soil are:

2.6.1 Direct design methods

Direct design methods are used to apply site-specific data, for instance, cone penetration test (CPT) findings. The CPT is recognized as a speedy and can repeated test that gives a consistent soil profile, allowing correlations between the cone's tip impedance, friction from sleeves on the shaft, and toe impedance. However, reduction factors must be applied to the measured CPT values in direct pile design to account for differences in insertion techniques, scale, where the CPT friction sleeve is located, loading rate, and displacement of soil horizontally [26].

Several direct design approaches that incorporate CPT results, such as the LCPC method, are available. In this section, The explanation of how to analyze CPT data can help determine the ultimate bearing capacity and soil shear strength. the interpretation of CPT data will be explained to estimate soil shear strength and ultimate bearing capacity. The CPT results are applied in The 'solitary' and 'cylindric' techniques, previously discussed, to estimate the the helical screw piles' bearing capacity. According to [5], soil's ultimate bearing capacity (q_{ult}) and shear strength (S) are determined by:

$$q_{ult} = q_{ca} k_c \quad (2.1)$$

$$S = q_s \quad (2.2)$$

Where, q_{ca} is defined as the equivalent cone tip impedance at the bottom of the helical flanges, determined as the total cone tip resistance 1.5 times the helical flange diameter from the tip,

k_c is considered the penetrometer bearing capacity factor, and

q_s is measured as the cuticle friction during the cone permeation test.

Such method is widely used for conventional piles to set ultimate bearing capacity [5].Laboratory Central des Points et Chaussées (LCPC) method is derived from investigations involving 197 static loading tests conducted at 48 sites, covering various pile kinds , inclusive conventional driven, drilled, and screw of piles. The data from the cone penetration test (CPT) will be used to forecast the ultimate bearing capacity and soil shear strength.

The border load (QL) of a deep down foundation is determined using the LCPC technique by adding the border lasing friction along the pile shaft (QLF) and the border impedance at the piling point (QLP).

“Equations (2.3) and (2.4)” are used to calculate the pile point resistance and total cuticle friction, respectively, for multi-layered formations when the cone tip impedance (q_c) is known “(Bustamante and Gianceselli, 1982)” [5].

$$Q_{LP} = q_{ca} \cdot k_c \cdot \frac{\pi(D_p)^2}{4} \quad (2.3)$$

$$Q_{LF} = \sum_1^i Q_{Li}^F = \sum_1^i q_{si} \cdot \pi \cdot D_p \cdot l_i \quad (2.4)$$

Where:

q_{ca} is defined as the equivalent cone permeation impedance below the helix/pile toe (with an average depth on par with 1.5 times the helix diameter/pile toe) (kN/m^2).

q_c is the cone penetration resistance obtained from the CPT (in units of stress).

k_c refers to the bearing capacity factor of a penetrometer.

D_p is the diameter of pile (m).

Q_{si} is the border unit of cuticle friction at the depth of layer i (kN/m^2).

L_i is the layer's thickness i (m).

Where The maximum pile capacity, is the aggregate of the pile point load and the total cuticle friction.[5] suggested that a safety factor of 2 be applied to cuticle friction and a safety factor of 3 be applied to point resistance in order to establish the allowed load for the pile. The CPT profile is used to calculate the equivalent cone resistance, or q_{ca} , in the following ways: Prior to doing anything further, the values of the cone tip resistance, or q_c , are first averaged over a length of $(+a)$ above the pile tip site to a distance of $(-a)$ below the pile tip location, where (a) is half the pile diameter. The equivalent cone resistance, q_{ca} , is estimated after the q_c profile is clipped; this average value is referred to as q'_{ca} (see Figure 2.6) By using this clipping, values more than $1.3 \cdot q'_{ca}$ may be removed along the distance below and above the pile point, and values less than $0.7 \cdot q'_{ca}$ above the pile point can be removed throughout the length (a) . In actuality, a computer can calculate the q_{ca} calculation processes for the raw data (an Excel sheet).

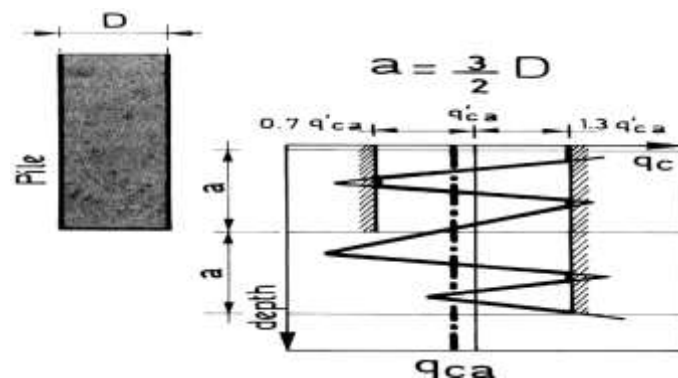


Figure 2.6: Procedure for Determining Equivalent Cone Impedance Using the LCPC process [5]

2.6.2 The theoretical design methods

Various theoretical design methods used to estimate the capacity of screw piles beneath both tension and compression loads are addressed within this section.

2.6.2.1 Cylinder shearing technique

In expansive soils, the cylindrical shear method has been adapted to account for the unique behavior of the soil, particularly the volume changes caused by moisture variations. Originally proposed for sand [30], the cylindrical shear failure model has been modified for use in expansive soils to determine the capacity of screw piles. A cylindrical shear failure surface is assumed to be formed between the bottom and top helices, with the bearing capacity defined by the lower plate for compression and above the upper plate for tension. Additionally, the soil-soil interaction (cylindrical shear) between the helices and the shaft-soil frictional resistance above the top helix is considered [61,25,44,45].

In expansive soils, as outlined by [36], equations for cylindrical shear failure are influenced by soil conditions, pile geometry, the number of plates, and the spacing between helices, as well as the swell potential of the soil. The failure mechanism of screw piles in expansive soil is impacted by the soil's swelling and shrinkage characteristics. Consequently, design adaptations have been made to the bearing and uplift capacity of screw piles in these soils, with emphasis placed on the expansive nature of the soil and its effect on the cylindrical shear surface [35].

The equations for bearing and uplift capacity in cohesionless soils, proposed by [30], have been modified for expansive soils by incorporating parameters such as soil swell pressure and moisture variation. These modifications are necessary because the internal friction angle, typically used for cohesionless soils, must be adjusted to account for the behavior of expansive soils, providing a more accurate analysis of screw pile performance under such conditions.

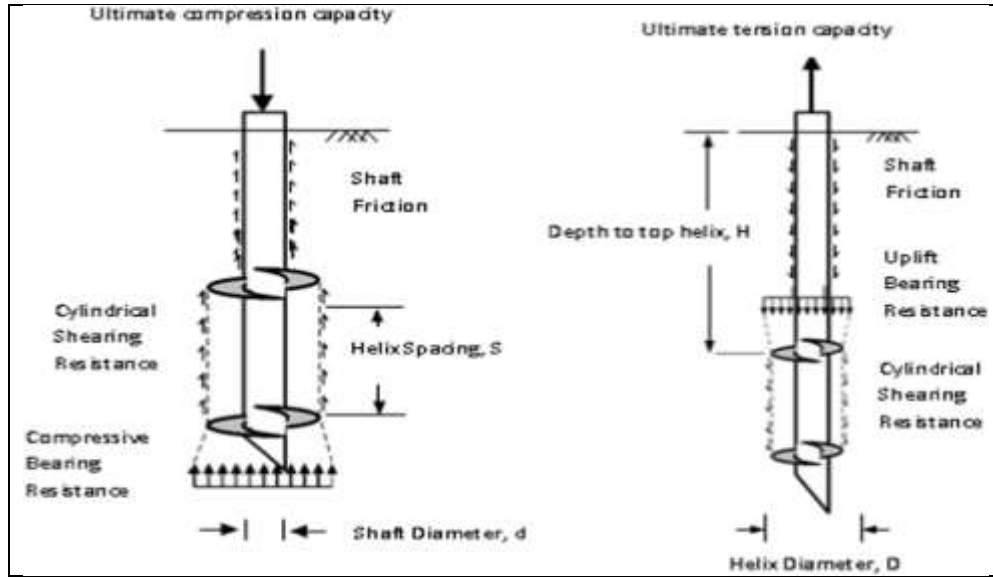


Figure 2.7: The Details of Cylindrical Shear Failure under Tension and Compression Loading [35]

The screw pile analysis provided by [30] is as follows:

$$Q_{com} = Q_{helix} + Q_{bearing} + Q_{shaft} \quad (2.5)$$

$$Q_{helix} = \frac{1}{2} \pi D_a \gamma (H_b^2 - H_t^2) K_s \tan \phi \quad (2.6)$$

$$Q_{bearing} = \gamma H A_h N_q \dots \quad (2.7)$$

$$Q_{shaft} = \frac{1}{2} P_s H_{eff}^2 \gamma K_s \tan \phi \quad (2.8)$$

$$Q_{com} = \frac{1}{2} \pi D_a \gamma (H_b^2 - H_t^2) K_s \tan \phi + \gamma H A_h N_q + \frac{1}{2} P_s H_{eff}^2 \gamma K_s \tan \phi \quad (2.9)$$

Symbol	Parameter
Q_{com}	Is defined as the total compressive (resistance) helical pile capacity.
Q_{helix}	The helix bearing capacity.
$Q_{bearing}$	The base (shaft) bearing capacity.
Q_{shaft}	The only shaft frictional resistance.
D_a	The total diameter for helix.
H_{eff}	The length of the effective helix above the top ($H_{eff} = H - D$).
H	The screw pile embedment depth.
D	The screw pile embedment depth.
d	The shaft diameter.
H_b	The distance to the bottom helix.
H_t	The distance to the top helix.
A_h	The lower helix surface area ($A_h = \pi r^2$, where r represents the helix radius).
K_s	The compression case's coefficient of lateral earth pressure (as shown in the table).

$$N_q = e^{\pi \tan \varphi} \tan (45 + \frac{\varphi}{2})^2$$

An equation for the extreme capacity of a helical pile has been proposed [35] for situations in which the indulgence ratio (H/D) is less than 5, indicating a shoaly state, with a shaft friction resistance being neglected.

$$Q_{com} = \frac{1}{2} \pi D_a \gamma (H_b^2 - H_t^2) K_S \tan \varphi + \gamma H A_h N_q \quad (2.10)$$

The uplift resistance of helical piles in cohesionless soils was presented by “Mitsch & Clemence (1985)”[30]. The key physical parameters influencing the design and analysis screw piles under tension and compression loads in cohesionless soils are considered to be spacing ratio (S/D), embedment ratio, and screw pile length above upper helix.

Equations pile's bearing and uplift capacity in cohesion less soils were provided by “Mitsch & Clemence (1985)”[30]. The distinction between the design and analysis of screw piles in coherent and cohesion less soils is depending on the internal friction angle of the soil, which is used for cohesionless soils instead of the undrained shear strength used for cohesive soils.

It was proposed [62] that that screw piles under tension and compression loads be classified as deep foundations if their embedment ratio is more than 5, and as shallow foundations if it is less than 5. Differences in the design and analysis equations for a screw pile capacity under tension and compression are noted depending on the failure mechanism. For the uplift capacity of screw piles, the bearing zone is extended from the top plate to the soil surface [33], while in deep conditions; the bearing zone is located beneath the surface. The critical embedment ratio is shown in Table 2.1.

For multiple-helice screw piles in shallow conditions, the condition $H/D < (H/D)_{cr}$ is applied.

$$Q_t = \frac{1}{2} \pi D_a \gamma (H_b^2 - H_t^2) K_S \tan \varphi + \gamma H A_h F_q \quad (2.11)$$

For screw piles with multiple helices under deep conditions, the condition $H/D < (H/D)_{cr}$ is applied.

$$Q_t = \frac{1}{2} \pi D_a \gamma (H_b^2 - H_t^2) K_u \tan \varphi + \gamma H A_h F_q * + \frac{1}{2} P_s H_{eff}^2 \gamma K_u \tan \varphi \quad (2.12)$$

Where:

K_u = the lateral soil pressure coefficient in the event of uplift for cohesionless soil (as detailed in Table 2.2).

Q_t = screw pile total uplift capacity.

F_q = breakout factor for expansive soil in shallow conditions (as shown in Figure 2.8 a).

F_q^* = breakout factor for expansive soil in deep conditions (as shown in Figure 2.8 b).

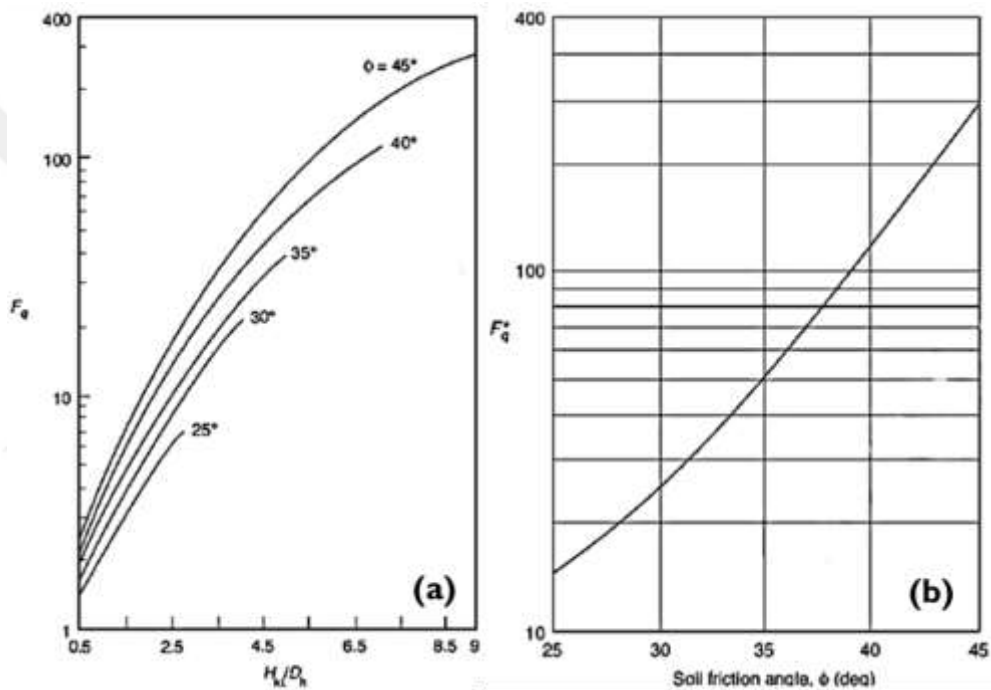


Figure 2.8: The Breakout Factor Variation for (a) Shallow Screw Piles and (b) Deep Screw Piles with Respect to Soil Friction Angle and the H_{ht}/D Ratio

Table 2.1: Critical Embedment Ratio, $(H/D)_{cr}$, is Presented in as Determined by [28]

The angle of Soil Friction, ϕ	The depth of critical embedded, $(H/D)_{cr}$
20°	2.5
25°	3
30°	4
35°	5
40°	7
45°	9
48°	11

Table 2.2: The uplift coefficients, K_u , for helical anchors, are shown in [30].

The angle of Soil Friction, ϕ	Coefficient for Uplift of Foundations by Meyerhof	Helical Anchor Coefficients Recommended
25°	1.2	0.7
30°	1.5	0.9
35°	2.5	1.5
40°	3.9	2.35
45°	5.3	3.2

2.6.2.2 Method of individual bearing

An equation for calculating uplift capacity was introduced by [51], according to helix diameter ratio to the shaft diameter, using non-dimensional factors. It was suggested by [1] that the screw pile capacity be determined according to the singular bearing method when the spacing between two adjacent plates is large. In this method, each helix is treated independently, resulting in individual bearing at each helical plate. Consequently, total bearing and uplift capacity of the screw pile is determined by average capacities of each helix, along with the shaft resistance [61,44,45,16].

Individual bearing mode is applied under both tension and compression loads in design and analysis. The screw pile capacity is influenced by the helix bearing area and the undisturbed soil beneath it under compression loading. For tension loading, the capacity is dependent on the helix bearing area and the disturbed soil above the helix. Equations for the individual bearing method involve summing the resistance of each helix, including the shaft resistance above the upper helix for deep screw piles. Equations (2.13) and (2.14), provided by [8], estimate screw pile capacity based on the sum of the individual bearing capacity of each helical plate, excluding shaft friction resistance.

For uplift capacity in cohesionless soil, Equation (2.9) was presented by [8], describing screw pile uplift capacity as the sum of the bearing capacities of each individual helix.

$$Q_t = \sum Q_h \quad (2.13)$$

Where

Q_t = Overall Uplift Capacity

Q_h = Bearing capacity of individual helix

$$Q_h = A_h q N_q = A_h \gamma H N_q \quad (2.14)$$

Equation (2.15) was proposed by [36] to describe the uplift resistance of screw piles, with shaft friction included. Additionally, Equation (2.16) was suggested [36] to explain screw pile capacity under compression loading.

$$Q_t = \sum Q_h + Q_{shaft} \quad (2.15)$$

$$Q_c = \sum Q_{bearing} + Q_{shaft} \quad (2.16)$$

$$Q_{bearing} = \gamma H A_h N_q$$

$$Q_{shaft} = \frac{1}{2} P_s H_{eff}^2 \gamma K_s \tan \varphi$$

γ = The dry unit weight of cohesion less soil

H = The depth of soil each every helix to surface

A_h = The surface area of helix

N_q = The break out factor for expansive soil (Table 2.3)

P_s = Shaft pile perimeter

H_{eff}^2 = The effective depth of soil

K_s = The coefficient of (Table 2.4)

φ = The internal friction angle of soil

Table 2.3: The Bearing Capacity Factor, N_q , for Cohesion Less Soils

The internal friction angle, φ	0°	5°	10°	15°	20°	22°	24°	26°	28°	30°	32°	34°	36°	38°	40°	42°
N_q	1	2	3	4	6	8	10	12	15	18	23	29	38	49	64	85

Table 2.4: The Typical Values of K_0 for Normally Consolidated Expansive Soil [17]

The Relative Of Density	K_0
Losse	0.4
Medium dense	0.5
Dense	0.6

According [7], it was proposed that K_s be considered equal to the coefficient of original earth pressure, K_0 , for bored piles, and twice the value of K_0 for driven piles.

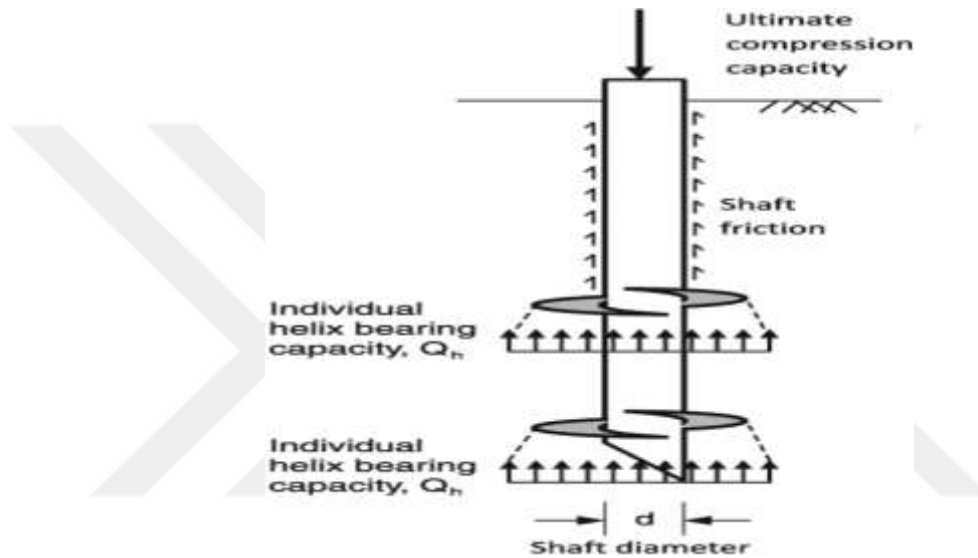


Figure 2.9: The Distribution of Force in the Singular Bearing Method for Screw Piles under Compressive Load Is Presented By [44]

2.6.3 Empirical approaches to design

The concept of linking installation torque to axial capacity for screw piles has been compared to the relationship between pile capacity and pile driving effort [18]. Empirical equations have been developed by several researchers to relate installation torque to the ultimate capacity of screw piles [13,34,18,40]. A direct empirical equation relating installation torque to screw pile uplift capacity was proposed by [18], as detailed in Eq. (2.17).

$$Q_t = K_t \times T \quad (2.17)$$

Where:

Q_u = The capacity of uplift (KN)

K_t = The factor of empirical (m^{-1})

T = The total installation of torque (kN·m)

In an analysis of 91 helical pile load tests from previous literature and the authors' private files, good approximations of screw pile capacity were acquired by [18] using K_t values of 33 m^{-1} for screw piles with square shafts and round shafts less than 89 mm in diameter, 23 m^{-1} for round shafts with a diameter of 89 mm, and 9.8 m^{-1} for round shaft piles with a diameter of 89 mm and 219 mm diameter extension shafts “extending from the upper plate to the surface”. The torque rapport suggested by “Hoyt & Clemence” provides empirical K_t factors for a bounded range of pile geometries. According to Equation (2.17), it was shown by [52] that total torque could be determined by averaging the last section of penetration (soil), which equals three times the diameter of the largest helix (i.e., $3D_h$).

Different limitations for the rapport between installation torque and screw pile capacity under tension and compression loads have been asserted by various research studies. It was explained by [44,45] that the correlations between installation torque and screw pile capacity were developed for small-diameter anchors that are exposed to uplift loads subjected to uplift loads, and therefore, caution should be exercised when applying these correlations to large-diameter piles.

The correlation moed was tested under compressive forces by [44], who concluded that due to differences in uplift and compressive failure mode mechanisms, as well as the non-uniformity of cohesionless soils near the upper and lower helical plates, the screw pile capacity under compression loads calculated from installation torque relations can't be used. Conversely, the correlation between installation torque and screw pile capacity under both compression and tension loads in cohesionless and cohesive soils was explicitly focused on [8].

$$F_t = \frac{T}{\gamma AHp} \dots (2.18) N_u = \frac{Q_u}{\gamma AH} \quad (2.19)$$

Where:

T = the final pile depth was measured by the installation torque (kN·m)

γ = expansive soil unit weight (kN/m^3)

A = helix surface area (m^2)

H = embedment depth pile (m)

p = the helix pitch distance (m)

Q_u = the uplift load ultimate (kN)

In 1991, it was shown by Ghaly and Hanna that a unique relationship existed between N_u and F_t for all types of screw piles with single-helix installed at varying depths into cohesion less soil, approximated by a logarithmic equation (2.2.).

$$N_u = 2F_t^{(1.1)} \quad (2.20)$$

The final uplift capacity in terms of the installation torque equation (2.21) may be predicted by applying Equations (2.18) and (2.19) to Equation (2.20).

$$Q_u = 2(\gamma AH) \left[\frac{T}{\gamma AH p} \right]^{(1.1)} \quad (2.21)$$

Based on the forces operating on a screw pile with a single helix, equation (2.21) was created. Additionally, the equation may be used for screw piles with multiple helices of constant pitch and diameter [13]. It was demonstrated by [13] that the force distribution in screw piles with multiple helices of constant pitch and diameter is essentially equivalent to that in screw piles with a single helix. It is discovered that the forces operating on a single-helix screw pile plate's upper surface are similar to those operating on a multi-helix screw pile plate's upper surface. Similarly, discovered the forces operating on the bottom surface of a single-helix screw pile plate are similar to those operating on the lower surface of a multi-helix screw pile plate.

2.7 Installation Torque Limitations

The various factors affecting the ultimate bearing capacity and empirical torque of piles were listed by [39] and [45]. These factors are pitch size, shaft size, spacing between helices, helix size, soil disturbance, embedment depth, pile configuration, groundwater levels, soil strength parameters, equipment calibration, and axial forces on the screw pile. It was noted that an enhancement in screw pile capacity is generally achieved with an increase in the number of helices, according to both the cylindrical shear and singular bearing modes . It was agreed upon by previous studies that an increase in installation torque is associated with larger helix diameters, greater helix thickness, and a higher number of helices. Should any of

these factors be increased without corresponding improvements to the screw pile material, such as an increase in shaft wall thickness, it is possible for the screw pile structure to be compromised, as higher torque values will be required to penetrate the soil.

2.8 Prediction Load Settlement Curve of Ultimate Capacity

The screw pile ultimate capacity is predicted using a variety of techniques based on the load-settlement curve's findings (static load testing). The ultimate uplift and compression bearing capacity of a screw pile is defined as the highest load that can be applied before a displacement increase occurs at the same applied load value. As illustrated in Figure 2.10, plunging failure loads may be observed for curves A and B, while plunging failure is not exhibited by curve C.

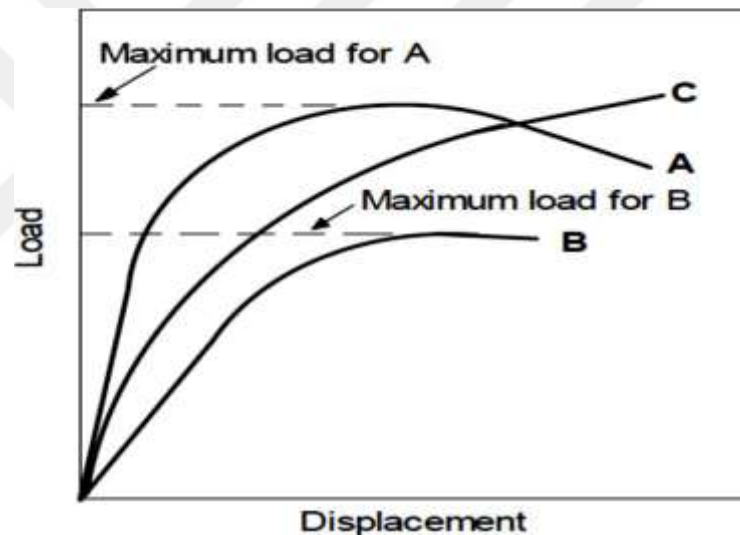


Figure 2.10: Typical Load-Displacement Curves [19]

Plunging failure is typically correlated with pile settlement values that significantly exceed the allowable settlement for structures. Three distinct regions can be observed at the load-settlement curve to the piles under axial compression and tension loads, as illustrated in Figure(2.9).

1- The first segment of linear elastic material, Which has a steep slope and high stiffness.

2-The non-linear region where the slope and stiffness gradually decrease.

3-The last linear section, Which has a lowly stiffness and a low slope.

The transfer of load from the pile head to the underlying soil is described in the first segment of linear elastic through a combination of shaft friction impedance and plate bearing strength. Within this area, the pile-soil system's global stiffness is kept constant. As the load increases in the transition zone, the friction impedance of the pile shaft is approached to its highest value, leading to the applied load being transferred to the soil through plate bearing, which results in non-linear global stiffness. Eventually, the highest friction impedance of the pile shaft is reached, and the ultimate bearing capacity contribution increases until its peak is approached. In this

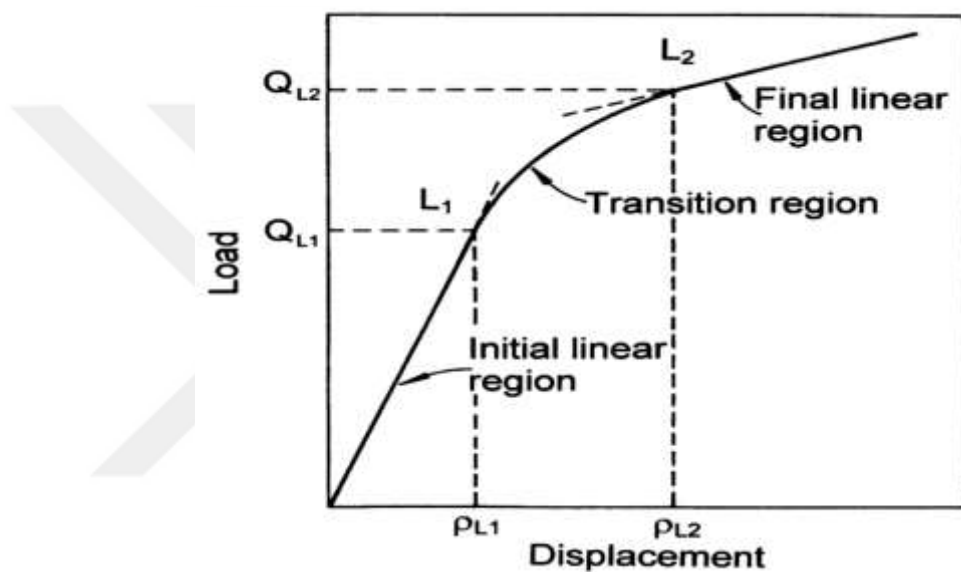


Figure 2.11: Curve Regions of Load Displacement [19]

Point, the ultimate bearing capacity of the pile is attained. Yet, beyond the transition zone, creep settlements significantly influence the pile's response, often causing fluctuating loads.

For this reason, the criteria for interpreting failure load are often designed to predict the ultimate capacity within the nonlinear transition region. The criteria should identify the upper and lower bounds of the transition zone, which correspond to points L1 and L2 [19], as shown in Figure (2.11). Broad criteria for interpreting failure load have been established.

- 1-The Fuller and Hoy methods was proposed by [12].
- 2-The O'Neil and Reese method was developed by [37].
- 3-Davisson's offset method was introduced by [10].

4-The slope and tangent method was presented by [6], along with other slightly modified versions.

5-A load at 10% of the helix diameter was suggested [44,45,60,36,61,49].

6-A load at 5% of the helix diameter was recommended by [45].

A criterion for estimating the ultimate load was formulated by [12]. According to this criterion, the point at which the load-settlement curve's slope hits 0.14 mm/kN (0.05 inches/ton) is known as the ultimate load. The point marks the onset of dipping and the corresponding ultimate bearing capacity.

The slope and tangent method [6] has been used to predict the ultimate bearing capacity of a pile. In this method, the ultimate bearing capacity is defined by the intersection of a straight line drawn through the first segment of linear elastic material and the tangent to the load-settlement curve in the last linear section, where the slope equals 0.14 mm/kN (0.05 inches/ton). The failure load and settlement value are interpreted within the non-linear portion of the load-settlement curve [6]. These two methods are recommended for estimating the ultimate load in the Quick Load test procedure [2]. "In Northern America, the offset limit load [10] is used, where the pile's settlement under the ultimate load is given by equation (2.22) [22].

$$S_p = \frac{QL}{E_p A} + \frac{D}{120} \quad (2.22)$$

Where:

S_p = the ultimate loading for total settlement pile head.

Q = load ultimate.

L = length of pile.

E_p = The pile material's Young's Modulus.

A = the effective area of the pile cross-sectional.

D = the diameter for toe pile it's given in(mm).

2.9 Previous Studies of Centrifuge and Small-Scale Anchor Models in Expansive Soil

The screw piles behavior and anchors in expansive soils has been the focus of several studies, often investigated through centrifuge or small-scale models to replicate real-world conditions.

Several centrifuge experiments on single-helix screw anchors embedded in expansive clay were conducted by [48]. It was revealed that the uplift impedance of screw anchors in expansive soil was significantly affected by moisture content and embedment depth. The expansive soil properties, such as swelling potential and soil suction, were shown to directly impact the ultimate uplift capacity, with higher moisture levels leading to a reduction in capacity.

Small-scale model tests in expansive soil were performed by [20] to investigate the interaction between screw piles and soil framing during swelling and shrinkage cycles. It was demonstrated that screw piles experienced cyclic uplift due to soil expansion, particularly as moisture content increased. It was also shown that embedment depth played a critical role in reducing the effects of expansive soil movements on pile stability.

Centrifuge modeling to examine the way multi-helix screw piles behave in expansive soils under varying moisture conditions was conducted by [23]. It was concluded that piles installed in drier conditions exhibited higher initial bearing capacity. However, as moisture was absorbed by the soil, causing expansion, the capacity of the screw piles decreased, particularly at shallower depths. The study emphasized that moisture conditions must be considered carefully during pile installation in expansive soils.

[55] Utilized centrifuge models to assess the performance of grouted screw piles in expansive clay. The outcomes indicated grout significantly enhanced the screw pile's resistance to uplift forces caused by soil swelling. The combination of screw piles with grouting was found to be particularly effective in reducing the impact of moisture variation on pile performance, as the grout provided additional frictional resistance between the pile and the expansive soil.

[24] Investigated effects of expansive soil properties on screw piles bearing capacity, using small-scale anchor models. It was observed index of plasticity and

moisture content of expansive soils had a strong influence on screw pile performance. Piles installed in soils with higher plasticity indices were more prone to cyclic uplift and settlement due to the expansive nature of the soil. Additionally, It was found that adding more helices increased the pile's capacity to resist vertical movements in expansive soils.

[63] Performed centrifuge experiments to analyze the helical screw performance anchors in expansive soils under cyclic loading. The research showed that repeated loading cycles caused cumulative damage to the soil-structure interface, resulting in a gradual reduction in uplift resistance over time. However, it was found that deeper embedment and larger helix diameters helped to mitigate these effects by distributing the load over a greater volume of soil.

These studies illustrate the challenges presented by expansive soils for screw pile and anchor installations, particularly due to the soil's sensitivity to moisture content and its propensity for significant volume changes.

3. THE PROCESS OF CENTRIFUGAL MODELING AND TESTING

3.1 Introduction

This chapter's goal is to examine the screw pile models' ultimate bearing and uplift capacities in expansive soil, which experiences large volume changes as a result of moisture fluctuations. Using a built centrifuge apparatus, the study examines how screw piles behave under various loading scenarios, such as tension and compression. Comparing the outcomes with traditional models, small-scale models, highlights how expansive soil conditions affect pile performance. Along with thorough explanations of each component of the centrifuge system, the chapter also describes how torque affects the bearing capacity of the screw pile in expanding soils. There are also detailed procedures for installing screw piles, preparing the soil, and applying other sorts of loads, such as tension and compression at different angles.

The French engineer Eduardo Philips identified in January 1869 the application of centrifuge modeling in civil engineering, recommending the use of this method for modeling a bridge's superstructure. Using this concept to geotechnical issues arose in the USSR in the years between World Wars I and II [47]. Its use was unknown elsewhere until the 1960, when Mikasa (Japan) and Schofield (Cambridge) realized its potential [9]. The International Society for Soil Mechanics and Foundation Engineering Conference in Mexico in 1969 saw the publication of the first papers pertaining to geotechnical centrifuge work since 1936.

Expansive soils, often referred to as swelling or shrinkage soils, show notable volume changes as a result of variations in moisture content, which creates difficulties for foundation designers. Geotechnical engineers can accurately simulate soil-structure interaction (SSI) and evaluate stiffness, bearing capacity, and overall stability under complicated loading situations by using centrifuge models to explore these concerns. These days, geotechnical centrifuges are frequently utilized to solve

issues with slope stability, earth retaining structures, and foundation systems in difficult soil types including expansive soil.

3.2 The Centrifuge Modeling Concept

The behavior of soil in geotechnical problems is nonlinear and is dependent upon the effective confining stress. The idea behind centrifuge modeling is to create an equivalent amount of stress in both the prototype and the model by increasing the "gravitational" acceleration of the physical models. Scaling stress is therefore necessary to meet the similarity requirements of geotechnical models in order to produce reliable data for intricate situations like soil-structure interaction. The physical application of Newton's Second Laws of Motion, which describe the rotation of mass around a fixed axis with a constant radius into a radial path at a certain angle and speed, is centrifuge modeling. The mass will experience an inward acceleration by the centrifuge in the direction of the rotational axis of:

$$a = \omega^2 r \quad (3.1)$$

Where:

ω = velocity of angular (rad/sec)

r = radius from rotational center (m)

The radial acceleration that is applied, \mathbf{a} , is

$$a = N g . \quad (3.2)$$

Where:

N = factor scaling of gravity

g = velocity brought caused by gravity (9.81m/s^2)

The angular velocity and radius from the center of rotation determine the radial acceleration. The model's self-weight stress increases as a result of the acceleration impact on the soil; as a result, the gravitational stresses in the prototype match the inertial stresses in the model. A mass of soil inside a container rotates around a fixed axis at a constant radius and angle speed in a centrifuge; as a result, the lateral acceleration equals N times the gravitational force, or what is known as the scaling factor.

The goal of the scaling rule is to ensure that the stress conditions of the relevant prototype and the model are equivalent. The soil in the prototype has a density of ρ at a depth of h_p . The vertical tension is represented by σ_{vp} , where p is the prototype.

$$\sigma_{vp} = \rho g h_p \quad (3.3)$$

The vertical stress (σ_{vm}) in the model at depth h_m is given by (where, m denotes to model) if the density of soil in the prototype and model is the same, according to centrifuge modeling theory.

$$\sigma_{vm} = \rho N g h_m \quad (3.4)$$

Thus,

$$\rho N g h_m = \rho g h_p \quad (3.5)$$

Therefore,

$$h_m / h_p = 1/N \quad (3.6)$$

Since the factor scale, N , for a linear dimension of the model to the prototype is (1: N), the displacement scale factor is also 1: N . The scaling factor for stress and its corresponding strain is 1:1, in turn. Stated otherwise, the inertial stress in the centrifuge model corresponds to the prototype's gravitational stress. The soil's vertical stress distribution in the model and related prototype is described in Figure (3.1). Figure (3.2) compares how the prototype and the model's stress variation changes with depth. Table (3.1) displays the scale factor of the model and prototype.

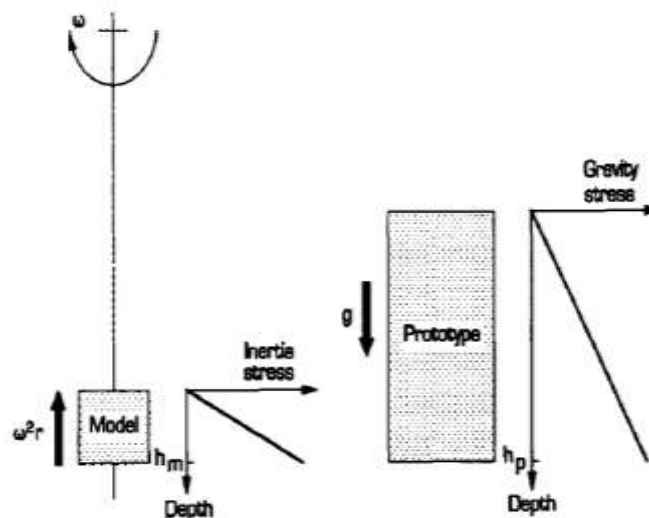


Figure 3.1: Describe How the Prototype and Model's Vertical Stress Distributions

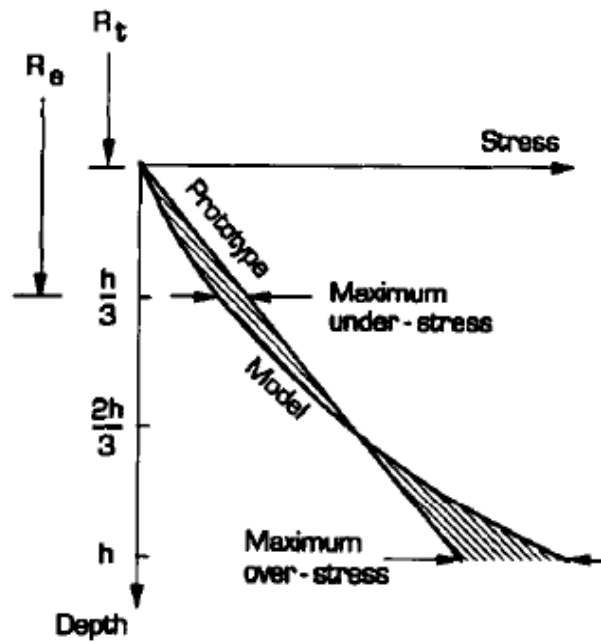


Figure 3.2: The Model and Prototype Are Compared In Terms Of How Stress Changes with Depth

Table 3.1: The Prototype and Model's Scale Factor

Quantity	Prototype	Model
Length	N	1
Area	N^2	1
Volume	N^3	1
Velocity	1	1
Acceleration	1	N
Mass	N^3	1
Force	N^2	1
Energy	N^3	1
Stress	1	1
Strain	1	1
Density of Mass	1	1

3.3 Parts and Equipment of Centrifuge Devices

3.3.1 The control board

Numerous electric switches on the control board may be used to send commands to the centrifuge system to supply electricity, adjust rotational velocity, and activate the main on/off switches. Figure3.1 displays the control board's specifications. The centrifuge device's orientation and rotational velocity are

manually controlled by the speed control of the AC Drive in figure 3.1a. In accordance with ASTM Specification D-1143, figure 3.1b illustrates the unique electric relays with timers that are utilized to convey the order to the first gearbox to apply compression and tension loads to the screw piles for a duration of five minutes during centrifuge testing.



Figure 3.3: Control Board Detail

3.3.2 The arm and rotation axis

Two axes make up the centrifuge system: the first axis is a shaft with a fixed base that is constrained from the top to maintain rotation stability. A primary gearbox with varying degrees of velocity can rotate the system's second axis, which is coupled to the first axis. There are two sections to the second axis, which symbolizes the arm of the centrifuge system. With a length of 1.70 meters, the first section allows cables that feed power to the load cell indicator, first gearbox, and second gearbox to pass. The second arm segment, measuring 1.70 meters in length, serves as an equilibrium component when the centrifuge system rotates, as seen in Plate (3.2).

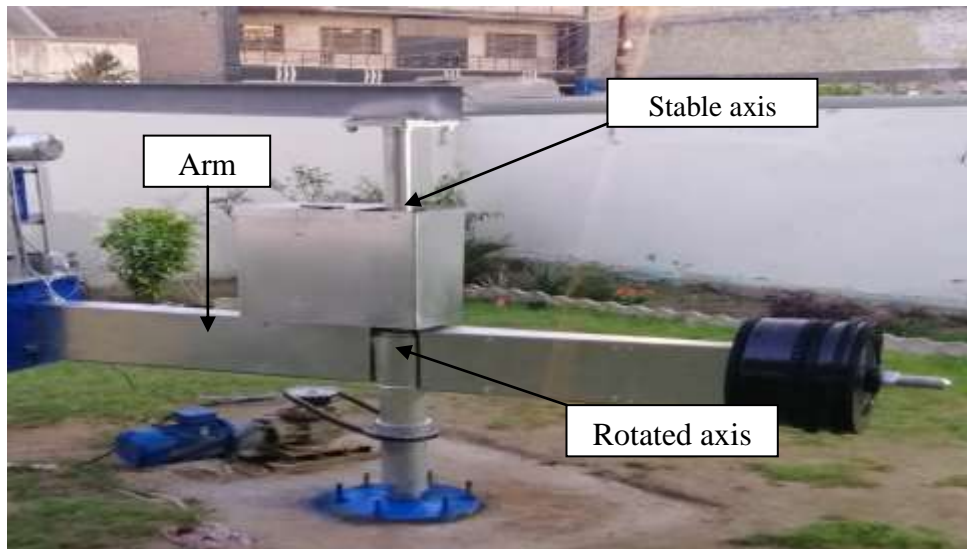


Figure 3.4: The Centrifuge Arm and Rotation Axis

3.3.3 The system's main gearbox

The primary gearbox's function is to rotate the centrifuge system by switching from gearbox movement to angular velocity created by a rotating axis. The control board's AC drive regulates the main gearbox's speed of movement and rotational rate. The Type SEW primary gearbox parameters and details are displayed in Table (3.2) and Plate (3.3), respectively.

Table 3.2: The Main Gearbox Properties

Description	value
Power	5.5 HP
Rpm (velocity of angular)	200
I (ratio of conversion)	9.6

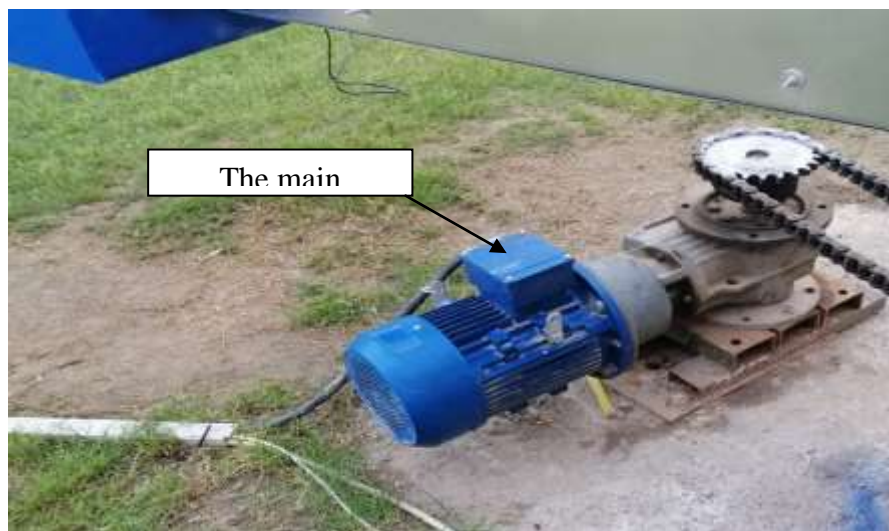


Figure 3.5: The Centrifuge System Main Gearbox

3.3.4 Soil container

The steel container, which measures 0.5 meters in length, 0.5 meters in width, and 0.5 meters in height, is held up by a frame, as seen in Plate (3.4). To prevent any deformation during the test, the container and centrifuge system arm are welded together.

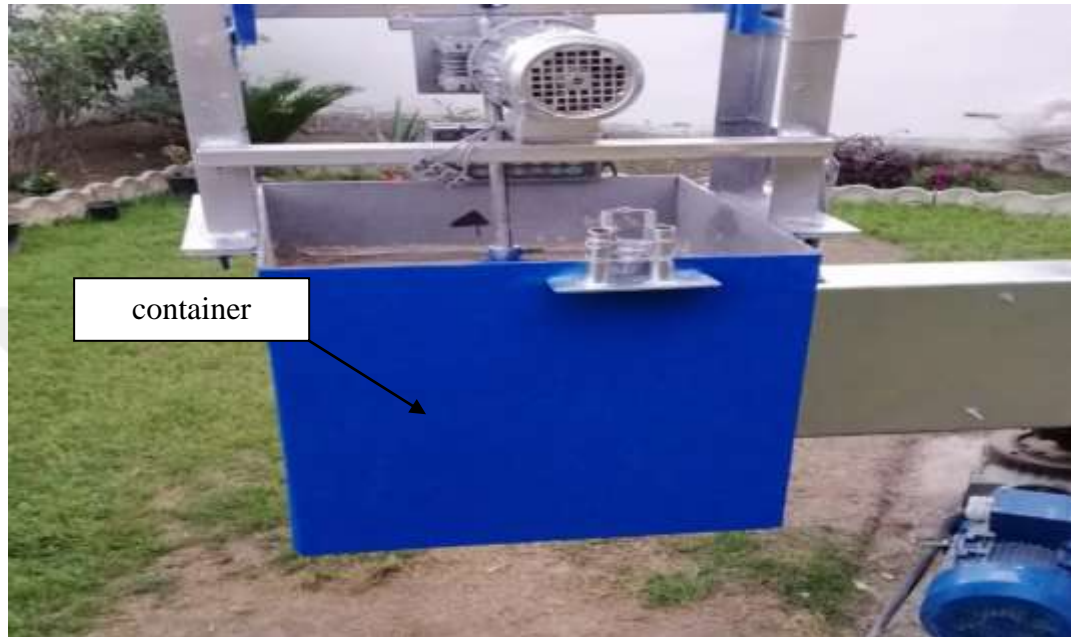


Figure 3.6: The Soil Container

3.3.5 Screw pile installation

According to [4], a hydraulic torque motor is used to advance the helical pile during the installation of pile model in the ground. Torque is applied at the head of the pile shaft to cause the helical pile to rotate and penetrate the soil [49]. According to [46], the installation torque values should only be used to subjectively evaluate the installation and should be utilized cautiously in the absence of a precise installation technique. As a result, the current study used a precise installation approach that takes into account the geometry of helical pile and the properties of the soil. First, Equations (2.5) to (2.12) are used to hypothetically forecast the helical pile's final capacity. The parameters employed in the equation were determined by the failure state (deep or shallow foundation) and the failure mechanism (individual bearing failure or cylindrical shear failure). The subsequent phase, as proposed [13], a reference for the first estimate of installation torque from capacity, is the ultimate capacity of the helical pile as a direct connection with installation torque for a 1-g model of Equation (3.7).

$$\left[\frac{Q_u}{\gamma AH} \right] = 2 \left[\frac{T}{\gamma AHp} \right]^{(1.1)} \quad (3.7)$$

Where Q_u is a helical pile's maximum bearing capacity, γ is the soil's unit weight, A is the area of helix's surface, H is depth of pile embedment, T is the torque installation at the final pile depth, and p is the pitch of helix. For various pile types, as shown in Table (3.3), the installation speed rate of rotation is defined based on the counterpart torque at 10-g, which is based on the mechanical parameters of the second gearbox as presented in Figure (3.3). As per the recommendations of earlier studies, the speed rate of rotation was maintained constant during the pile construction to provide a vertical movement equal to one time the pitch of the helical pile helix every revolution [40,53]. To minimize ground disturbances during installation, the helical pile's vertical movement velocity per rotation should be more than 0.85 times the pitch [41]. With varying pitch values, the penetration rate of helical piles varies. For instance, the earth is penetrated by helical piles with a pitch of 6 mm at a vertical movement rate of 6.0 mm/revolution. The first and second gearbox details are displayed in Table (3.4 a, b). The first and second gearboxes are seen on figure(3.4) and (3.6), respectively.

Table 3.3: The Torque and Rotational Speed for Some Helical Piles Installation

Model helical pile designation	2HD 40P0	2HD 40P3	2HD 40P5	2HD 40P7	2HD 40S1	2HD 40S1. 5	2HD 40S4	2HD 40S6	1HD 40
Speed rate of rotation (rpm)	15.2	10.5	11.7	14	9.8	8.6	12.1	14.6	16.4
Installation torque (N.m)	103	145	131	111	155	175	127	107	96

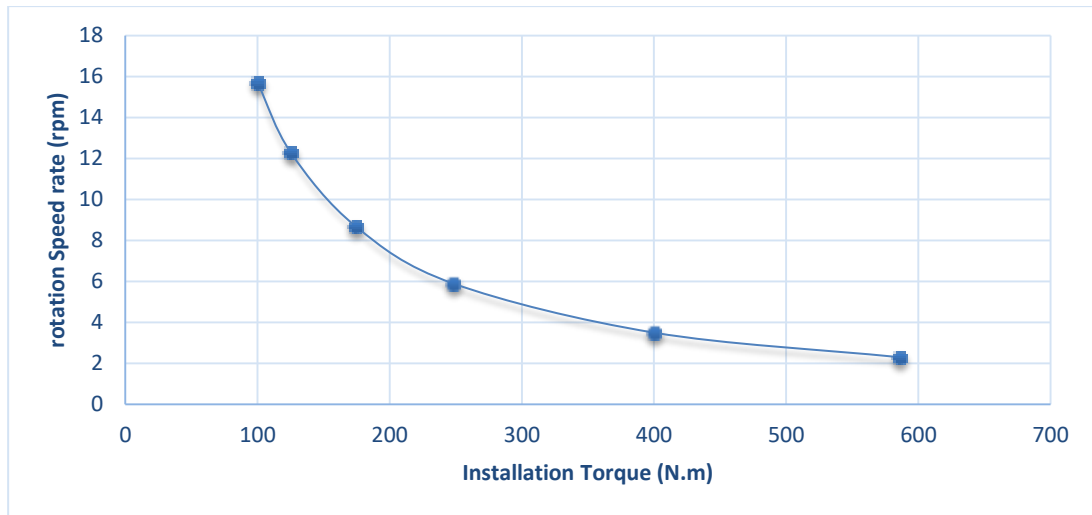


Figure 3.7: The Relationship between Torque Speed and Rotation Rate

Table 3.4: The First and Gearbox Details, Respectively

Description	value
Power	0.5 HP
Rpm (angular velocity)	16
I (conversion ratio)	1/100

a

Description	value
Power	0.25 HP
Rpm (angular velocity)	25
I (conversion ratio)	1/80

b



Figure 3.8: First Gearbox

3.3.6 The results obtaining and monitoring

The results are transferred wirelessly from the measuring instrument, which is fixed within the container during rotation, via video recording. An additional electronic device receives the produced findings over the internet, allowing for full test process monitoring and control.

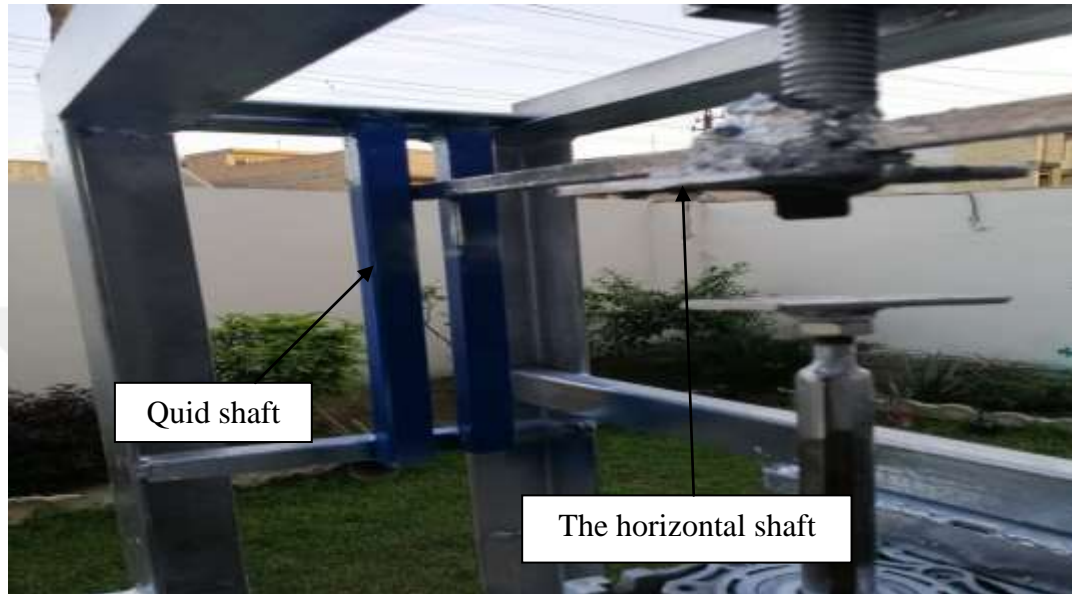


Figure 3.9: Described the Horizontal Shaft's Movement inside the Quid Steel



Figure 3.10: The Cell Load



Figure 3.11: The Indicator Digital

3.4 Measuring Settlement

The settling of screw pile models was measured using two dial gauges. There is a mechanical dial gauge and a digital dial gauge. The goal is to assure the correctness of the results recorded by using two dial gauges to monitor the outcomes using two separate devices. Two-dial gauges are shown in figure 3.10.



Figure 3.12: The Two Dial Gauges

3.5 Models of Screw Pile

A steel shaft of 20 mm in diameter and 1.5 mm in thickness was used to create 23 screw pile models. The steel shaft was welded using helical plates that had

varying thicknesses (2 mm) and diameters (40, 50, and 60 mm). Two distinct helical numbers, single and multi-helix, were employed in this investigation. The distance that the helix plate was welded to the steel shaft varied according to the spacing ratio, that is, the difference in the diameter and pitch of the helix, as well as the distance between two helices. Investigating how a screw pile's capacity responds to tension and compression loads is the goal.

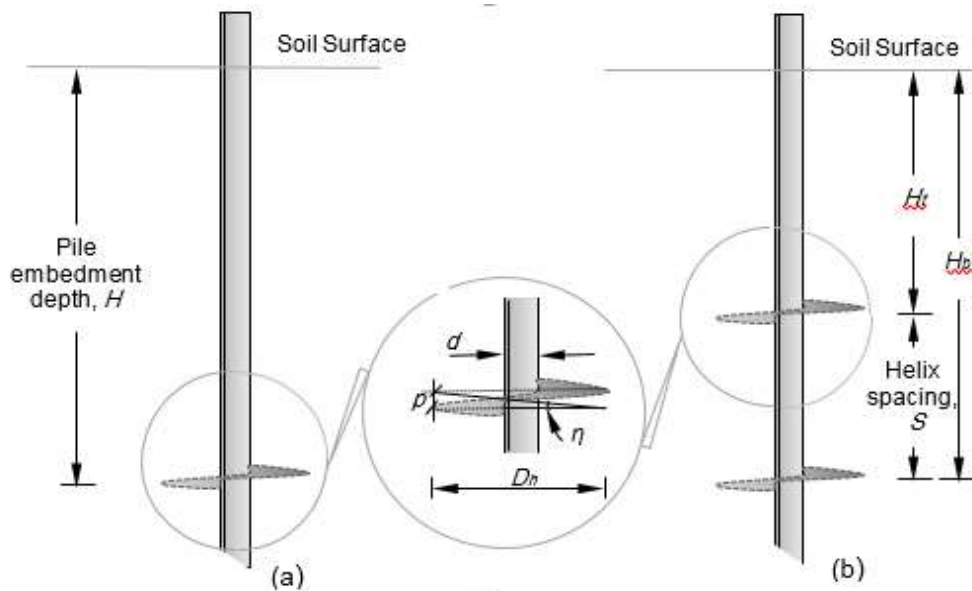


Figure 3.13: The Screw Pile Models' Dimensions and Configurations In

3.6 Procedure of Testing

The process of testing for screw pile models may be broken down into the following steps:

1-Soil is prepared inside a container using the method previously demonstrated in this chapter; the density of the soil depends on its relative density. A steel plate is then placed over the soil's surface to prevent it from escaping the container when the centrifuge system rotates.

2-To guarantee that the screw pile model is upright during the soil penetration as indicated in figure (3.12), the screw pile model was fixed with the shaft of the second gearbox.

3- The torque required to drive the helical pile determines the rotation speed (rpm) of the second gearbox.

4-According to the British Standards Institution Code of Practice (BS 5918:1980), the horizontal shaft of the first gearbox descends with a vertical distance, v , of $(0.85 \text{ pitch} < v < 1.15 \text{ pitch})$ each revolution, until it comes into touch with the shaft of the second gearbox. Screw pile models will pierce the soil by the combined actions of the first gearbox falling and the second gearbox rotating. Figure (3.13) illustrates the screw pile installation.

5- The first gearbox's horizontal shaft is raised to place a load cell between it and the second gearbox's shaft once the screw pile installation procedure is complete.

6- Installed all the equipment (dial gauge, electronic device, and load cell) in the proper locations. As figure (3.14) shows, the load cell is positioned between the first gearbox's horizontal shaft and the second gearbox's shaft.

7- Silicon paint is applied to the borders of the soil cover, which is a square steel plate. Figure is an example of this (3.15).

8- The control board (manual speed control of AC drive) regulates the centrifuge system's rotational velocity, which is based on the scaling factor value N .

9- A timer relay in the control board controls the application of load and the direction of movement of the first gearbox's horizontal shaft.

10-Using an external electrical device to monitor the test and document the applied load and helical pile settling findings.



Figure 3.14: Second Gearbox and the Fixating Screw Pile



Figure 3.15: The Installation Screw Piles

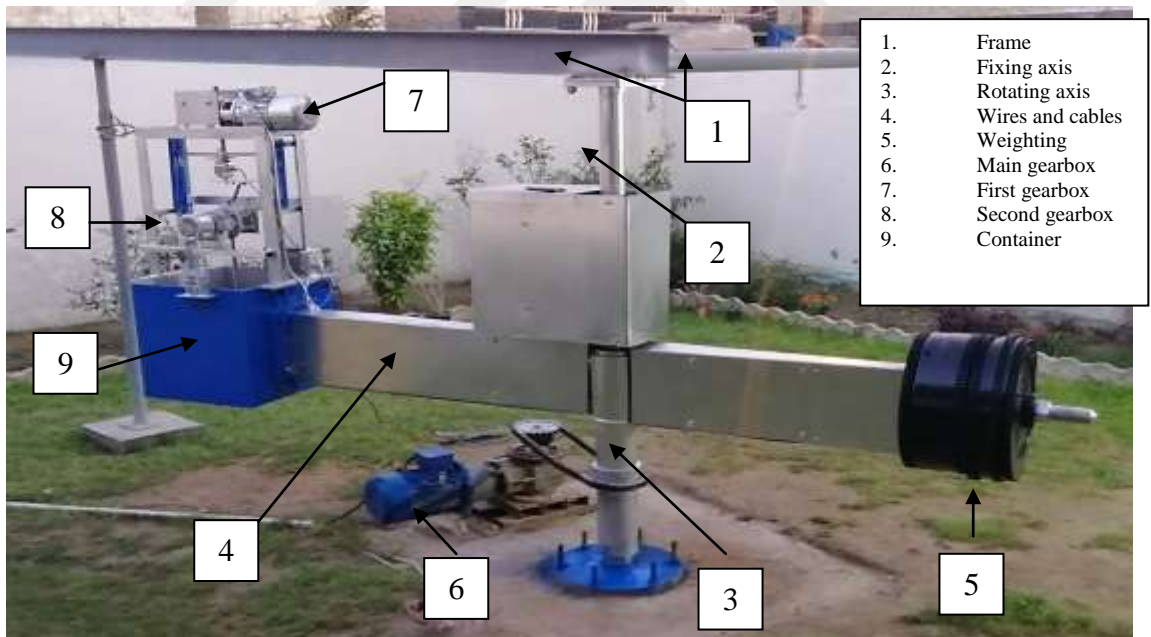


Figure 3.16: The Painting of the Soil-Covered Plate



Figure 3.17: The System Centrifuge

3.7 Testing Program for Foundations in Expansive Soil

- In the first group, one model of a foundation was tested in expansive soil without any special considerations for soil swelling (control group).

- In the second group, five foundation models were embedded in expansive soil with varying initial water content levels (0%, 5%, 10%, 15%, 20%), and the impact of moisture variation on the soil's swelling behavior and its effect on foundation performance was studied.

- In the third group, five models with different embedment depths (0.5D, 1D, 1.5D, 2D, 2.5D) were used to analyze how deeper foundations respond to the upward pressure caused by soil swelling in expansive soil.

- The fourth group focused on the effect of foundation geometry, with single, double, and triple plate models tested. These models, with helix diameters equal to 2D, were embedded in expansive soil under similar moisture conditions, while the spacing ratio (S/D) was kept constant at 3.

- In the fifth group, foundation models with varying diameters (2D, 2.5D, 3D) were embedded in expansive soil to observe how the size of the foundation influences its performance under swelling conditions.

- In the sixth group, the effect of inclination under tension was examined by testing one foundation model at different angles (30°, 60°, and 90° to the horizontal). The spacing ratio (S/D) was kept constant at 3, and the foundation's diameter was

equal to $2D$.

- In the seventh group, two foundation models were tested under compressive loads with spacing ratios (S/D) of 1.5 and 3. The pitch distances were equal to $0.3D$, and the helix diameters were $2D$, allowing the effects of soil swelling and lateral confinement to be studied.

Note:

- Except for the fifth group, all tests were conducted under both compression and tension forces.

- All tests were carried out using centrifuge modeling as well as small-scale modeling, with the exception of the seventh group, which was tested under relative densities of 55% and 75%.

- The foundation models were 300 mm in length, except in one case (foundation with three helices and a diameter of $2.5D$), where the length was 350 mm.

Figures and plates illustrate the applied load orientations and overall testing configurations. The verification of the geotechnical centrifuge system was conducted by estimating the ultimate bearing capacity of a shallow foundation (prototype footing of $1.0\text{ m} \times 1.0\text{ m}$) and comparing this result with the stress characteristics method.



Figure 3.18: An Inclined Load



Figure 3.19: A Vertical Load

3.8 The Scale Effect of Expansive Soil on Foundation Models

The impact of soil expansion on shaft resistance and the swell pressure delivered to foundation bearing regions are the two main processes taken into account when addressing scale effects in centrifuge model tests on foundations in expansive soils. The behavior of expansive soil and the ratio of the foundation diameter to the average particle size of the soil (d/D_{50}) usually account for the first mechanism, which is associated with soil expansion. Scaling effects are reduced in expansive soils when d/D_{50} is higher than 50, as Fioravante (2002) showed in sandy soils. This suggests that particle size has no discernible impact on foundation behavior at these ratios. Because the d/D_{50} ratio employed in this investigation is far higher than 70, scale effects on shaft resistance can be regarded as insignificant.

The results of Ovesen (1979) [38] on scale effects in sand apply to expansive soils for the second mechanism, which deals with the bearing capacity of the foundation under swelling pressures. Ovesen showed that when the diameter of the foundation is greater than 30 times the typical particle size ($30D_{50}$), scale effects become negligible. The pressure created by soil swelling in expansive soils is crucial to the functionality of the foundation. With a foundation diameter of 40 mm, a D/D_{50} ratio of 142 has been used for the foundation model in this investigation. Because the bearing and swelling resistance of the foundation are both correctly

represented at this scale, the impact of scale effects on centrifuge tests is thus regarded as insignificant for expansive soils.

3.9 3 D Plaxis Software Program

A finite element program called PLAXIS 3D was created especially for the analysis of flow, stability, and deformation in geotechnical engineering applications. Complex finite element models may be quickly generated thanks to the straightforward graphical input processes, and the improved output facilities offer a thorough display of the computational findings.

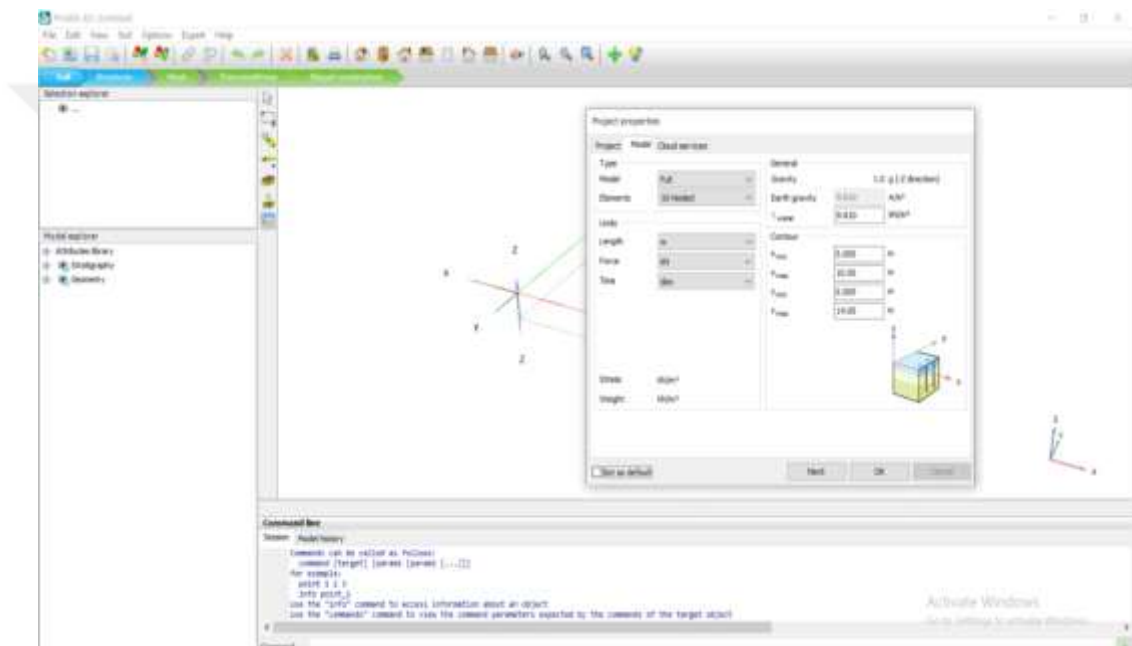


Figure 3.20: Project Properties Window in PLAXIS 3D

4. METHODOLOGY

4.1 General

This chapter presents and discusses the findings from the (64) test of screw pile models. The parameters that impact the screw piles' bearing capacity behavior are used to categorize the test results of the screw pile models. The following factors are taken into account: pitch distance, spacing ratio (S/D), helix number, helix diameter, and the kind of applied (tension and compression) load on the screw pile. All tests were performed using expansive soil samples with moisture content in the presence of groundwater in the surface soil layer at a depth of 1 m. The experimental procedures used established methods for determining swelling pressure and soil deformation, such as ASTM D4546 [3] for measuring the swelling potential of soils and methods described in Holtz and Kovacs [17] for evaluating soil properties.

4.2 The effect of Materials on the Experimental Results

The observed performance of the helical piles was greatly affected by the material that was used in the experimental models. The piles were made of steel, which is very strong and rigid to ensure that it is stable during centrifuge loading. These tests were done in expansive soil which has a high potential of swelling due to changes in moisture content. The homogeneous preparation of the soil also contributed to homogeneity in the swelling and shrinkage behavior, and the steel piles reduced the structural deformation. Hence, it was found that the differences in the bearing capacity were caused by geometric and interaction of the soil with the structure instead of material inconstancy.

4.3 Numerical Modeling

The objectives of this research are to simulate the behavior of helical piles using 3D Plaxis (Plaxis 2020) software, the load-bearing capacity of helical, and the effect of the distance between the screws on the distance of the screw and helix

formation. In this part, helical pile models were put through both compression and tension tests in expansive soil. The water level has been observed at a height of 0.5 meters above the soil surface. The objectives of this research are to simulate the behavior of helical piles using 3D Plaxis (Plaxis 2020) software, the load-bearing capacity of helical, and the effect of the distance between the screws on the distance of the screw and helix formation. In this part, helical pile models were put through both compression and tension tests in expansive soil. The water level has been observed at a height of 0.5 meters above the soil surface. posed of the expansive soil with the characteristics of the properties, which is defined by a unit weight (γ) of 18 kN/m³ and an internal friction angle (ϕ) of 33°, and the layer has a depth of 4 meters. Under this, second layer (preceded by sand), a unit weight (γ) of 19 kN/m³ and internal friction angle (ϕ) of 32°, have been designated to a depth of 10 meters. The pile, designed with 40 cm diameter and 12.7 mm thickness is designed out of steel. Helix plates, of the same material- steel- have also been supplied with different diameters of 30 cm, 40, cm, 50 cm, and 60 cm and the same thickness of 25.4 mm. The length of the pile as a whole has been figured at 3.5 meters. There is also an input $U_x = 0.1$ displacement. Pitch distance (0.5 d), S/D the spacing ratio 1 to 3 has been used on the pile. These specifications have been defined in a manner so as to obtain clarity and excellence of the drawn structural elements and their properties.

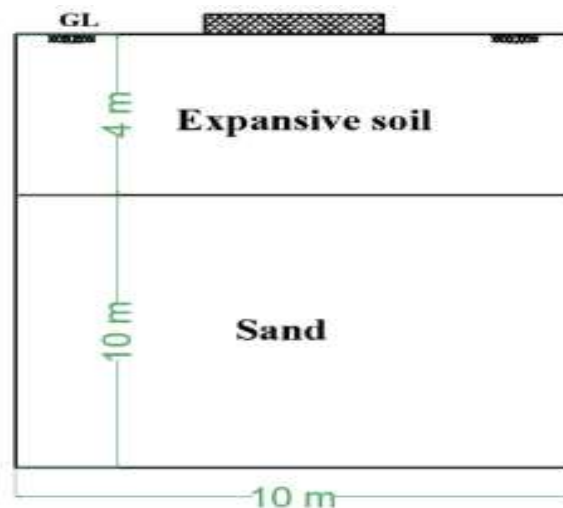


Figure 4.1: Expansive Soil Layer Overlying Sand Layer in a Soil Profile

Table 4.1: The Soil Parameters for Expansive Soil and Sand (Undrained Behavior)

Model parameter		Expansive soil (Undrained behavior)	Sand (Undrained behavior)
Symbol	Soil parameters		
γ_{unsat} (kN/m ³)	Unsaturated unit weight	18	19
γ_{sat} (kN/m ³)	Saturated unit weight	18	19
E_{50}^{ref} (kN/m ²)	Reference secant stiffness	3200	40000
E_{oed}^{ref} (kN/m ²)	Reference tangent stiffness	3200	40000
$E_{ur}^{(ref)}$ (kN/m ²)	Reference unloading-reloading stiffness	9600	120000
C' (kN/m ²)	Cohesion	18	0.01
ϕ' (°)	Internal friction angle	33	32
Ψ (°)	Dilatancy angle	0	0
v_{ur} (-)	Unloading/reloading poisson's ratio	0.2	0.3
m (-)	Exponential power	1	0.5

4.4 The Effect of the Screw Pile Model's Spacing Ratio S/D

The screw pile model was tested with one helix and two helices with pitch (0.5d), the diameter of the helix is (0.3m) and the relative density of the soil is (%). Figure (4.1) shows the bearing capacity of the screw pile with the diameter of a helix (0.2m) under the compression load effect of the spacing with different ratios of S/D for the small-scale model. Table (4.1) displays the bearing capacity of the screw piles with different spacing ratio S/D.

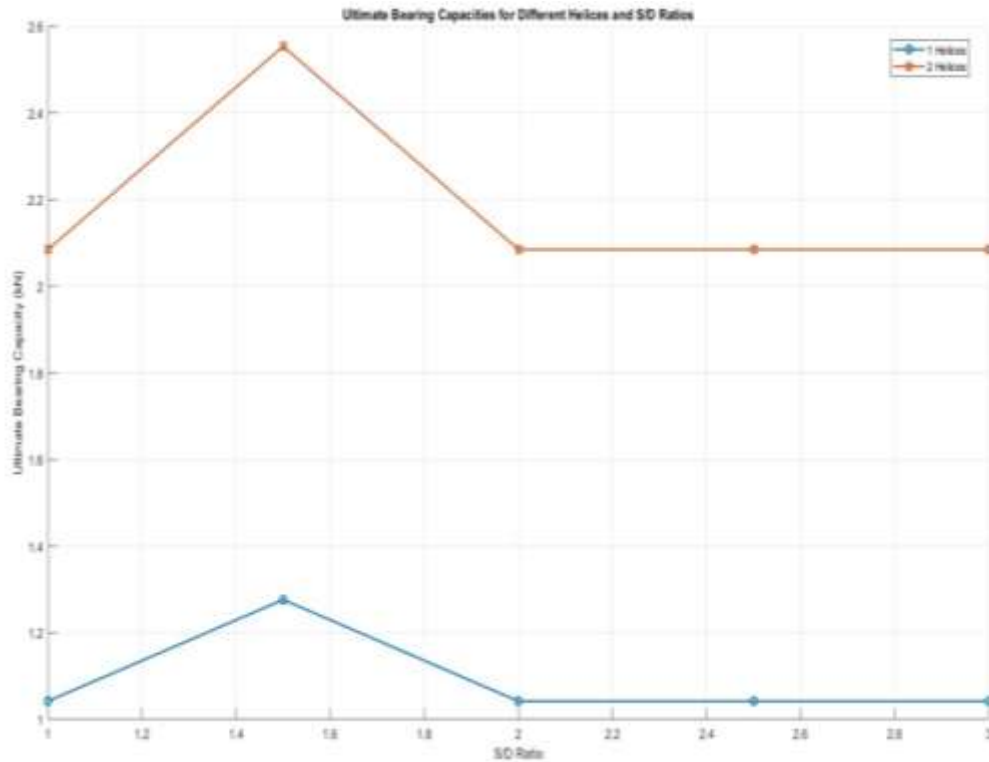


Figure 4.2: The Ultimate Bearing Capacities for Screw Piles with one Helix and Two Helices When Helix Diameter (0.3m)

Table 4.2: The Screw Pile Model's Bearing Capacity with Different S/D Spacing Ratios

S/D Ratio	Diameter of (1 and 2 helices) (m)	1 Helices Capacity (kN)	2 Helices Capacity (kN)
1.0	0.3	1.05	2.09
1.5	0.3	1.30	2.58
2.0	0.3	1.05	2.09
2.5	0.3	1.05	2.09
3.0	0.3	1.05	2.09

The figure displays the Ultimate Bearing Capacities for screw piles with one or two helices and different spacing-to-diameter ratios (S/D ratios). The relationship is explained in detail below:

4.4.1 Impact of S/D ratio on bearing capacity

It is found that the S/D ratio, which is the distance between helices compared to the diameter of each helix, plays a role in how well the load is spread through the helices into the surrounding soil.

From figure 4.2:

The maximum load that can be supported by one helix increases slightly at a ratio of S/D at 1.5 but as the ratio increases, the load-carrying capacity reduces and levels off. In all S/D ratios, piles of two helices will always exhibit better load bearing capacity than those of one helix meaning that the more the helix, the better the performance. However, when the S/D ratio is 1.5, the maximum load capacity of the double helix configuration is reached and thereafter, the capacity is almost constant before it starts to decrease slowly.

4.4.2 Comparative trends

The ultimate bearing capacity of a single-helix pile starts at around 1.05 kN, peaks at around 1.3 kN as the S/D ratio reaches 1.5 at which point it starts decreasing back to about 1.05 kN as the ratio becomes larger. The double-helix pile, on the other hand, has a greater initial capacity of approximately 2.09 kN, maximal capacity of approximately 2.58 kN at an S/D ratio of 1.5 then decreases slightly after this point until they stabilize to 2.09 kN at an S/D ratio of 3.0 and above.

All S/D the ratios show significant increases in bearing capacity when the helix diameter is raised to 0.4 m. The information that follows is a summary of how the spacing-to-diameter ratio (S/D) affects the performance of the screw pile:

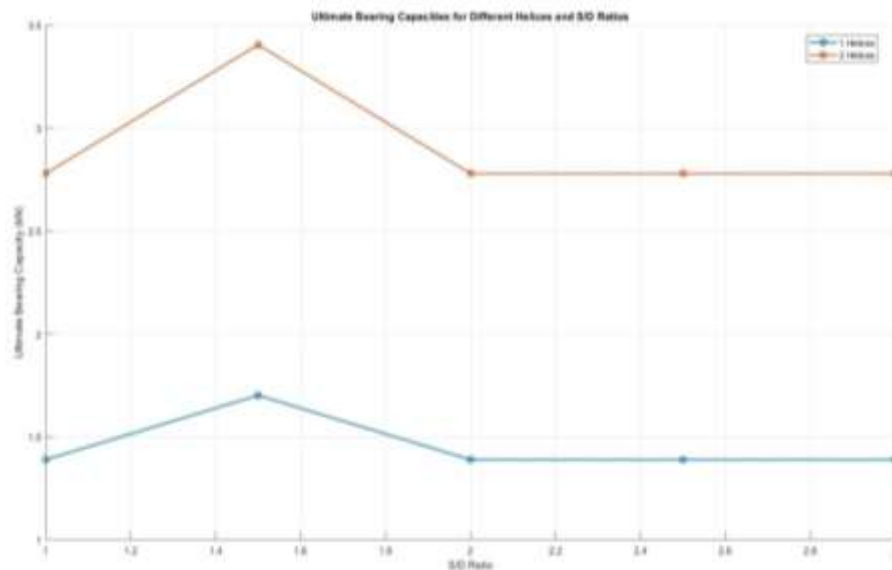


Figure 4.3: The Ultimate Bearing Capacities for Screw Piles with One Helix and Two Helices When Helix diameter (0.4 m)

Table 4.3: From the Inputs and Results for Diameter = 0.4m:

S/D Ratio	Diameter of (1 and 2 helices) (m)	1 Helix Capacity (kN)	2 Helices Capacity (kN)
1.0	0.4	1.4	2.8
1.5	0.4	1.75	3.4
2.0	0.4	1.3	2.8
2.5	0.4	1.3	2.8
3.0	0.4	1.3	2.8

The difference between single-helix and double-helix piles is a vivid demonstration of the effect of the number of helices on the load bearing capability of piles. In the case with the single-helix set-up, the highest possible bearing capacity was determined to be 1.87 kN at $S/D = 1.0$, with the highest possible bearing capacity being 2.32 kN at $S/D = 1.5$. The capacity dropped off beyond this spacing ratio, reaching a level of 1.87 kN, and this implies that $S/D = 1.5$ was the ideal spacing to allow the efficient transfer of loads. It is possible to explain the decrease in capacity at higher spacings in terms of poorer load distribution, since the helices interaction is reduced.

In the two-helix structure, an increased total capacity was noticed. Its initial value was 2.8 kN at $S/D = 1.0$ which reached a maximum of 3.4 kN at $S/D = 1.5$. In the same manner, as spacing increased beyond that of the single-helix case, the capacity started to decrease, the capacity reaching 2.8 kN. The enhanced performance of the two-helix pile demonstrates the added value of the extra helix in terms of load transfer but the performance becomes inefficient with increase in spacing ratio.

The results above, both constructions showed their best performance at $S/D = 1.5$ with the two helices pile having a constant higher bearing capacity than the single helix pile.

The bearing capacity of screw piles with a helix diameter of 0.5m is significantly influenced by the spacing-to-diameter ratio (S/D). The following observations have been made:

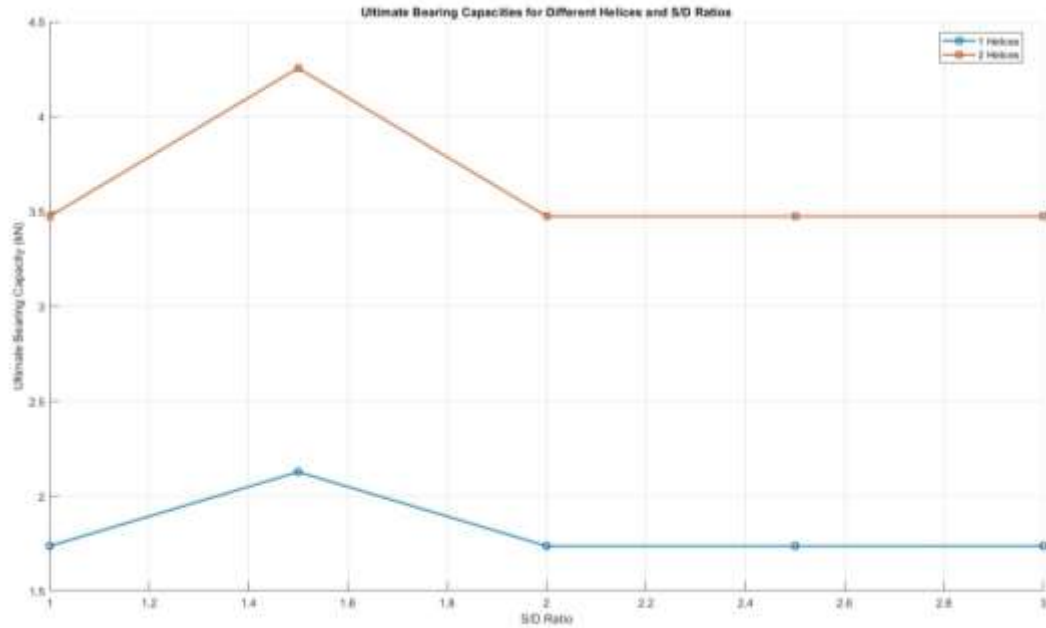


Figure 4.4: The Ultimate Bearing Capacities for Screw Piles with One Helix and Two Helices When Helix Diameter (0.5 m)

Table 4.4: From the Inputs and Results for Diameter = 0.5m

S/D Ratio	Diameter of (1 and 2 helices) (m)	1 Helix Capacity (kN)	2 Helices Capacity (kN)
1.0	0.5	1.75	3.49
1.5	0.5	2.20	4.25
2.0	0.5	1.75	3.49
2.5	0.5	1.75	3.49
3.0	0.5	1.75	3.49

The experimental outcome shows that the performance of the piles in load bearing is distinctly different in single-helix and in the case of the double-helix piles. In the case of single-helix, the bearing capacity rose at $S/D = 1.0$ with a value of 1.75 kN, reaching a high point of 2.20 kN at $S/D = 1.5$. After this, the decline was noted and the capacity was stabilized at a level of about 1.50 kN when S/D ratios were more substantial. This fact shows that the value of $S/D = 1.5$ is the most efficient load transfer in the situation of a single-helix.

The two-helix configuration, in its turn, demonstrated a much higher performance. The measurement of the capacity was 3.49 kN at $S/D = 1.0$ and a maximum of 4.25 kN at $S/D = 1.5$. Like the single-helix pile, the capacity changed downwards beyond the peak and stabilized at 3.49kN in greater spacing ratios.

In general both designs reached their maximum efficiency at $S/D = 1.5$ and the two-helix pile always offered better bearing capacity than the single-helix pile.

When the bearing capacity of screw piles with a helix diameter of 0.6m is significantly influenced by the spacing-to-diameter ratio (S/D). The following observations were made:

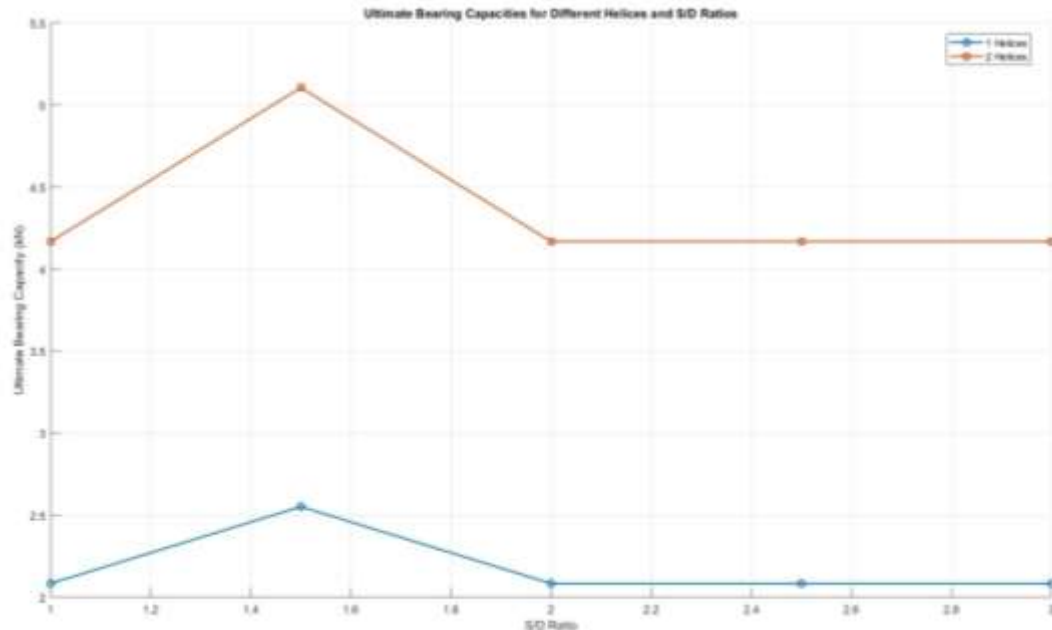


Figure 4.5: The Ultimate Bearing Capacities for Screw Piles with One Helix and Two Helices When Helix Diameter (0.6 m)

Table 4.5: From the Inputs and Results for Diameter = 0.6m

S/D Ratio	Diameter of (1 and 2 helices) (m)	1 Helix Capacity (kN)	2 Helices Capacity (kN)
1.0	0.6	2.10	4.20
1.5	0.6	2.56	5.10
2.0	0.6	2.10	4.20
2.5	0.6	2.10	4.20
3.0	0.6	2.10	4.20

The findings show conclusively the effect of the helix number on piling bearing capacity. In the case of the single-helix design, the capacity was found to reach its highest at 2.56 kN at $S/D = 1.5$ at the highest value of 2.10 kN at $S/D = 1.0$. On top of this spacing, there was a decrease and the capacity leveled at about 2.10 kN when the S/D ratios were large. This proves that $S/D = 1.5$ is the ideal spacing bandwidth to facilitate effective transfer of loads in the single-helix pile.

In the case of the double-helix, the overall capacity was higher. The initial weight on the pile was 4.20 kN therefore $S/D = 1.0$ and the highest weight was reached at $S/D = 1.5$ and was 5.10 kN. As in the case of single helix, the capacity declined beyond the peak to 4.20 kN at longer spacing ratios.

To conclude, both setups attained their optimum performance at $S/D = 1.5$ and the double-helix pile was able to sustain almost twice the bearing capacity of the single-helix pile.

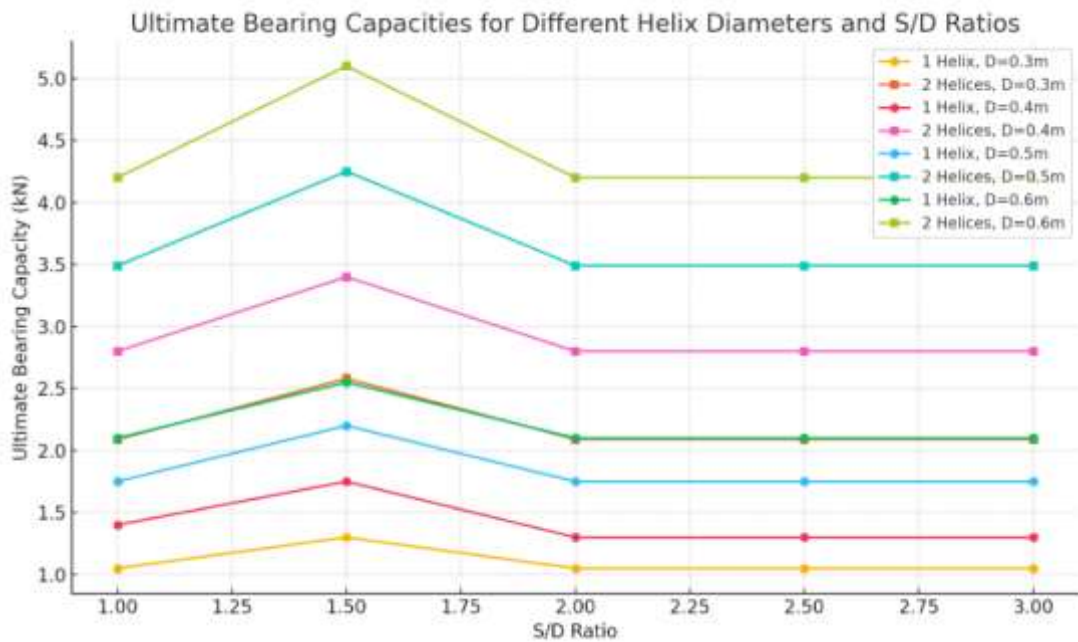


Figure 4.6: The Updated Bearing Capacity Results for Helix Diameters of 0.3 m, 0.4 m, 0.5 m, and 0.6 m with Different S/D Ratios

From the results, the bearing capacity and stability at various (S/D) ratios determine which helix diameter is best for screw piles in expansive soil. The smallest diameter, 0.3 m, had the lowest bearing capacity; a 0.4 m diameter showed a slight improvement. The 0.5 m diameter showed a notable increase in bearing capacity, peaking at $S/D = 1.5$ before stabilizing. Noting the variation in stability values, the 0.6 m diameter was found to have the maximum bearing capacity. Thus, a helix diameter of 0.6 m is advised if maximum bearing capacity is the primary goal, and a 0.5 m diameter is thought to be the best choice if stability and efficiency are to be balanced.

4.5 Percentage Change in Bearing Capacity by S/D Ratio

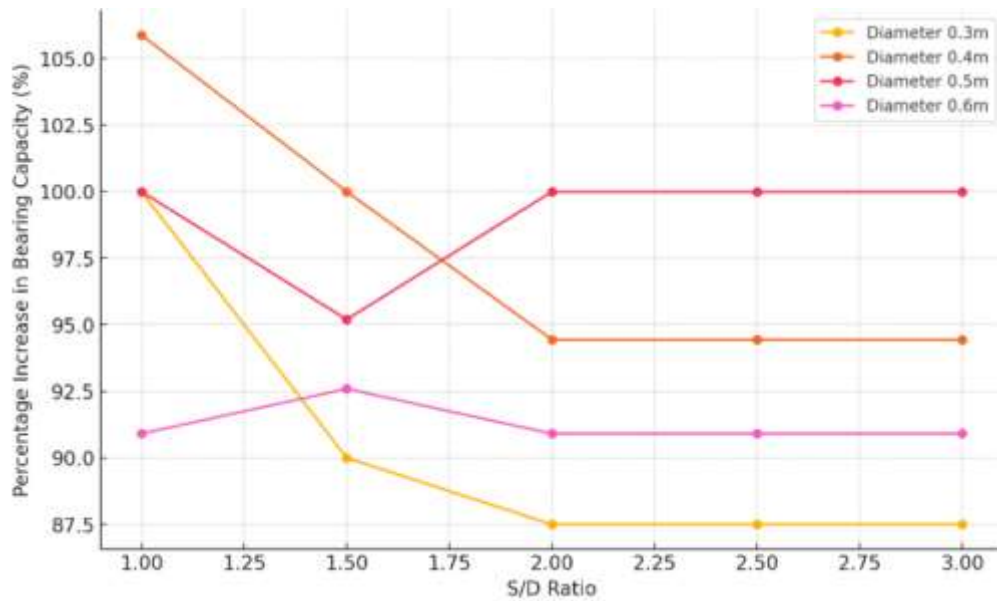


Figure 4.7: Percentage Increase in Bearing Capacity (%) Relative to S/D Ratio

The impact of adding more helices to screw piles has been investigated for a range of S/D ratios and helix diameters (0.3, 0.4, 0.5, and 0.6 meters). For all diameters, it has been found that adding a second helix greatly increases bearing capacity, with percentage increases ranging from 87.5% to 105.9%.

- At lower S/D ratios, a larger percentage increase has been observed for smaller diameters (0.3 and 0.4 m), whereas a slight decrease has been observed as the spacing increases.
- The percentage increase has stayed largely constant for larger diameters (0.5 and 0.6 meters), especially for S/D ratios greater than 2.0.

According to these results, a second helix increases load-bearing capacity, but its effect diminishes as the spacing-to-diameter ratio increases. A 0.4m diameter at S/D = 1.0 has shown the largest percentage increase (105.9%), while a 0.3m diameter at S/D = 2.0 and higher has shown the lowest increase (87.5%).

Table 4.6: The Percentage Increase in Bearing Capacity

S/D Ratio	Diameter 0.3m(%)	Diameter 0.4m(%)	Diameter 0.5m(%)	Diameter 0.6m(%)
1.0	100.0	105.9	100.0	90.9
1.5	90.0	100.0	95.2	92.6
2.0	87.5	94.4	100.0	90.9
2.5	87.5	94.4	100.0	90.9
3.0	87.5	94.4	100.0	90.9

4.6 Effect of Pitch Distance Screw Pile Model

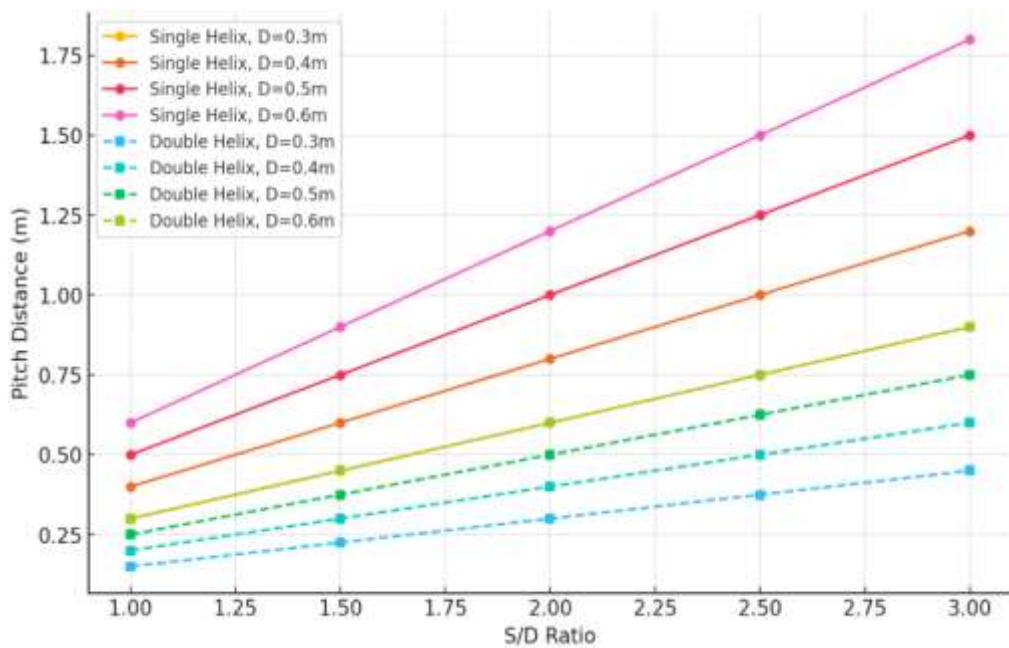


Figure 4.8: Pitch Distance vs. S/D Ratio for Single and Double Helix Screws

Table 4.7: The Pitch Distances (m) for Different Helix and Diameters

S/D Ratio	Diameter (m)	Pitch (Single Helix) (m)	Pitch (Double Helix) (m)
1.0	0.3	0.3	0.15
1.5	0.3	0.45	0.225
2.0	0.3	0.6	0.3
2.5	0.3	0.75	0.375
3.0	0.3	0.9	0.45
1.0	0.4	0.4	0.2
1.5	0.4	0.6	0.3

Table 4.7: (Cont.) The Pitch Distances (m) for Different Helix and Diameters

S/D Ratio	Diameter (m)	Pitch (Single Helix) (m)	Pitch (Double Helix) (m)
2.0	0.4	0.8	0.4
2.5	0.4	1.0	0.5
3.0	0.4	1.2	0.6
1.0	0.5	0.5	0.25
1.5	0.5	0.75	0.375
2.0	0.5	1.0	0.5
2.5	0.5	1.25	0.625
3.0	0.5	1.5	0.75
1.0	0.6	0.6	0.3
1.5	0.6	0.9	0.45
2.0	0.6	1.2	0.6
2.5	0.6	1.5	0.75
3.0	0.6	1.8	0.9

Based on the chart figure, it can be easily seen that the higher the S/D ratio, the closer the pitch distance. The pitch distance has a great influence on the performance of the screw conveyors and systems. The consequence of this is the following effects:

1. Material Flow Rate:

- With longer pitch distance, it is able to carry more material within a single revolution.
- When a two helix is applied, the flow is split between the two helices resulting in a smoother, and more continuous flow.

2. Inclination Handling:

- As the pitch distance increases, an even steeper grade can be used before fallback of material.
- Vertical transport normally prefers a smaller pitch in order to reduce slippage.

3. Power Consumption:

- The larger the pitch distance, the higher the pitch needs more torque because more material is being moved per pitch.

- The load is less in a single helix system and hence power consumption is also decreased to move a similar volume of transport load.

4. The process of compaction and mixing:

- A smaller pitch distance become more compact, useful in some applications like the extrusion.
- The bigger pitch makes mixing materials better because the distance between one screw and another is greater.

4.7 Effect of S/D Ratio on Load-Settlement

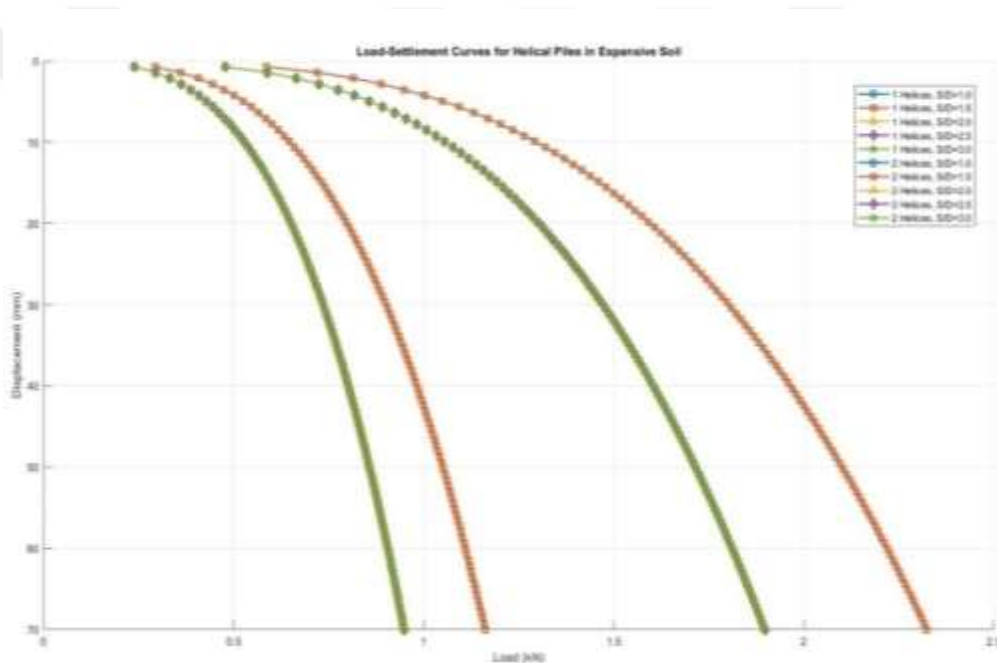


Figure 4.9: Load Settlement Curves for Helical Piles When Diameter (0.3m)

The provided figure illustrates the load-settlement behavior of helical piles in expansive soil for various S/D ratios (1.0, 1.5, 2.0, 2.5, and 3.0) and different numbers of helices (one and two helices). The displacement (mm) has been plotted against the applied load (kN) to evaluate the performance of screw piles under different configurations.

Table 4.8: Load-Settlement Values for Different S/D Ratios and Helix Numbers when Diameter (0.3m)

S/D Ratio	1 Helix - Ultimate Load (kN)	1 Helix - Settlement (mm)	2 Helices - Ultimate Load (kN)	2 Helices - Settlement (mm)
(1.0,2.0, 2.5,3.0)	0.251	0.772	0.301	0.772
	0.526	10.0	0.635	10.0
	0.647	20.0	0.802	20.0
	0.729	30.0	0.896	30.0
	0.805	40.0	0.973	40.0
	0.852	50.0	1.044	50.0
	0.898	60.0	1.106	60.0
	0.953	70.0	1.164	70.0
1.5	0.482	0.772	0.578	0.772
	1.057	10.0	1.293	10.0
	1.299	20.0	1.602	20.0
	1.459	30.0	1.805	30.0
	1.602	40.0	1.966	40.0
	1.709	50.0	2.108	50.0
	1.815	60.0	2.215	60.0
	1.901	70.0	2.326	70.0

Effect of S/D Ratio on Load-Settlement when diameter of helix (0.4m).

When the diameter of the helix was enlarged from 0.3 meters to 0.4 meters, the effect of the S/D ratio on the load-settlement behavior was influenced as follows:

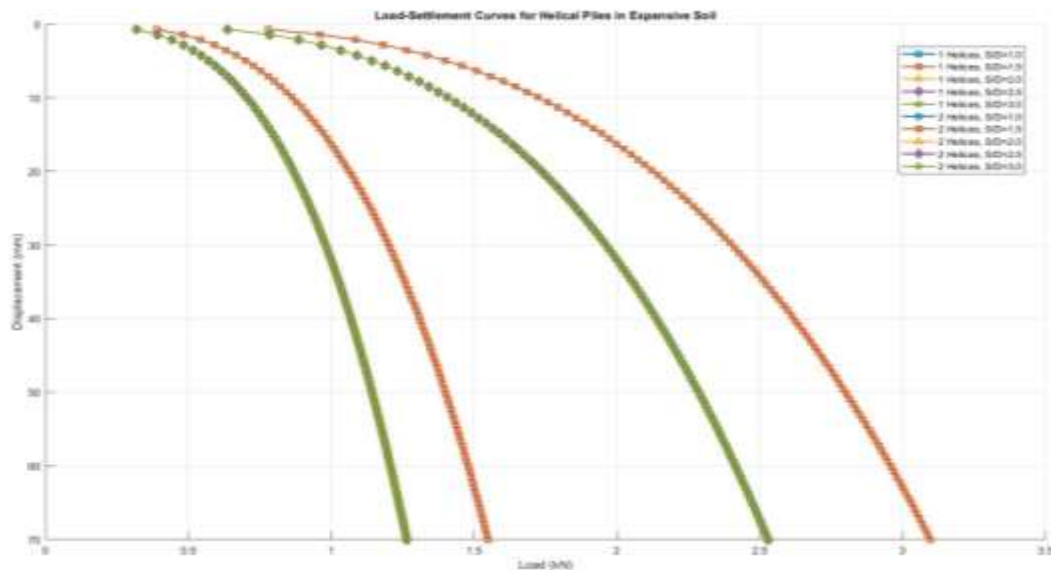


Figure 4.10: Load Settlement Curves for Helical Piles When Diameter (0.4m)

Table 4.9: Load-Settlement Values for Different S/D Ratios and Helix Numbers When Diameter (0.4m)

S/D Ratio	1 Helix - Ultimate Load (kN)	1 Helix - Settlement (mm)	2 Helices - Ultimate Load (kN)	2 Helices - Settlement (mm)
(1.0,2.0, 2.5,3.0)	0.319	1.148	0.638	1.090
	0.704	10.0	1.401	10.0
	0.865	20.0	1.730	20.0
	0.979	30.0	1.958	30.0
	0.805	40.0	2.131	40.0
	1.068	50.0	2.280	50.0
	1.208	60.0	2.415	60.0
	1.266	70.0	2.529	70.0
1.5	0.391	1.234	0.780	1.090
	0.858	10.0	1.716	10.0
	1.059	20.0	2.120	20.0
	1.201	30.0	2.399	30.0
	1.308	40.0	2.614	40.0
	1.398	50.0	2.790	50.0
	1.481	60.0	2.955	60.0
	1.549	70.0	3.099	70.0

Effect of S/D Ratio on Load-Settlement when diameter of helix (0.5m).

When the diameter of the helix was increased to 0.5 meters, the following effects on the load-settlement behavior were observed:

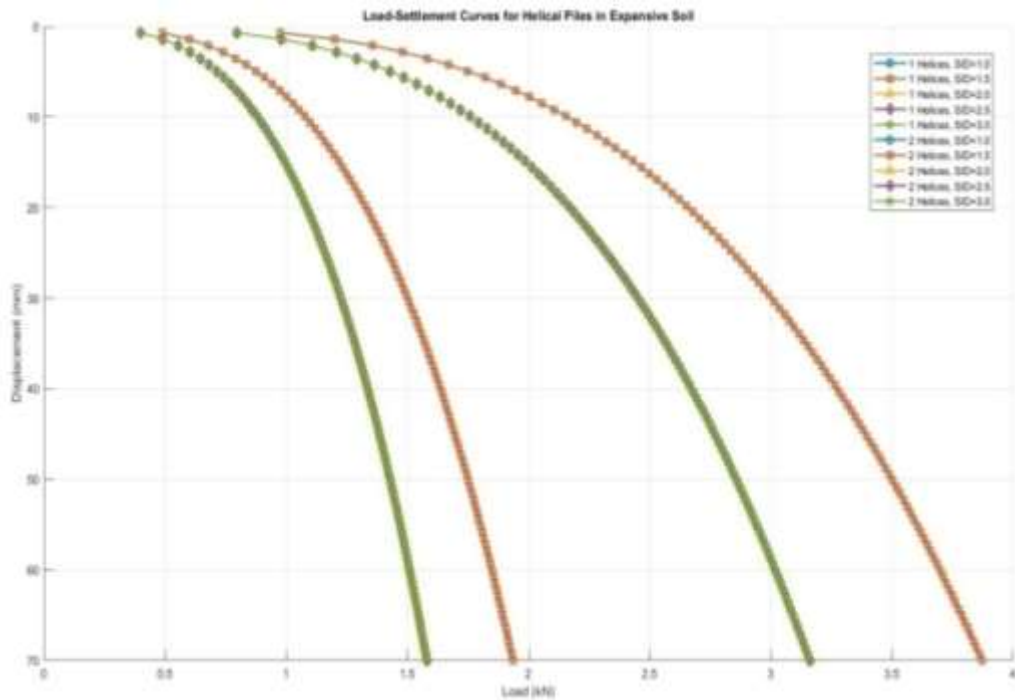


Figure 4.11: Load Settlement Curves for Helical Piles When Diameter (0.5m)

Table 4.10: Load-Settlement Values for Different S/D Ratios and Helix Numbers when Diameter (0.5m)

S/D Ratio	1 Helix - Ultimate Load (kN)	1 Helix - Settlement (mm)	2 Helices - Ultimate Load (kN)	2 Helices - Settlement (mm)
(1.0,2.0, 2.5,3.0)	0.408	0.289	0.804	0.3181
	0.885	10.0	1.762	10.0
	1.097	20.0	2.177	20.0
	1.233	30.0	2.458	30.0
	1.344	40.0	2.674	40.0
	1.435	50.0	2.858	50.0
	1.514	60.0	3.019	60.0
	1.588	70.0	3.161	70.0
1.5	0.495	0.289	0.981	0.202
	1.080	10.0	2.156	10.0
	1.331	20.0	2.667	20.0
	1.507	30.0	3.006	30.0
	1.641	40.0	3.274	40.0
	1.751	50.0	3.502	50.0
	1.851	60.0	3.654	60.0
	1.941	70.0	3.870	70.0

Effect of S/D Ratio on Load-Settlement when diameter of helix (0.6m)

When the diameter of the helix was increased to 0.6 meters, the following effects on the load-settlement behavior were observed:

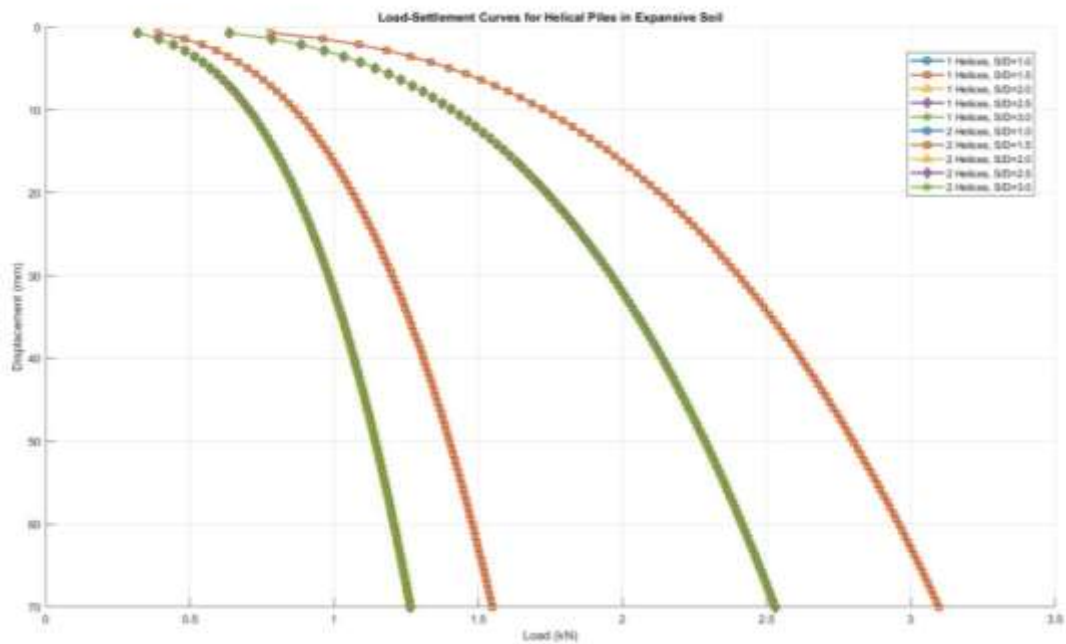


Figure 4.12: Load Settlement Curves for Helical Piles When Diameter (0.6m)

Table 4.11: Load-Settlement Values for Different S/D Ratios and Helix Numbers When Diameter (0.6m)

S/D Ratio	1 Helix - Ultimate Load (kN)	1 Helix - Settlement (mm)	2 Helices - Ultimate Load (kN)	2 Helices - Settlement (mm)
(1.0,2.0, 2.5,3.0)	0.489	0.405	0.9667	0.521
	1.071	10.0	2.119	10.0
	1.314	20.0	2.615	20.0
	1.480	30.0	2.951	30.0
	1.611	40.0	3.216	40.0
	1.722	50.0	3.436	50.0
	1.821	60.0	3.629	60.0
	1.904	70.0	3.798	70.0
1.5	0.597	0.289	1.182	0.550
	1.310	10.0	2.591	10.0
	1.605	20.0	3.199	20.0
	1.813	30.0	3.613	30.0
	1.974	40.0	3.934	40.0
	2.109	50.0	4.204	50.0
	2.228	60.0	4.443	60.0
	2.333	70.0	4.650	70.0

Load-settlement data for helical piles with varying diameters (0.3m, 0.4m, 0.5m, and 0.6m) and different S/D ratios is provided in the document. The key observations are as follows:

4.7.1 Increase in diameter leads to improved load capacity

As the diameter is increased from 0.3m to 0.6m, an increase in the ultimate load capacity for both single and double helices is observed.

A larger bearing area is provided by greater diameters, which enhances the soil-pile interaction and results in a reduction in settlement under a given load.

4.7.2 Effect of S/D ratio on load-settlement

The final load-settlement characteristics depend upon the S/D Ratio (Spacing/Diameter). The growth in the load capacity usually occurs when S/D increases and the settlement decreases at that load.

Lower ratios of S/D result in greater settlement, wherein higher ratios result in greater load resistance with reduced settlement.

4.7.3 Load-settlement behavior for different diameters

- With a Diameter of 0.3m: Lower load failure values are incurred as compared to larger diameter.
- With a Diameter of 0.4m: There is a small enhancement of load bearing capacity and a decreased settlement rise.
- Considering a Diameter of 0.5m: Great enhancement of the resistance of the loads on them was observed, especially where they were designed to have two helices.
- With a Diameter of 0.6m: Maximum load capacities and minimum settlement at a certain the load is realized.

4.8 Comparison of Results with Previous Studies

The outcomes of this experiment are consistent with the results of another study done by Ghaly and Hanna (1991) which determined a direct correlation between installation torque and ultimate bearing capacity of helical piles. Likewise, Perko (2009) noted that adding more helices will increase the load resistance to a considerable amount, and the same was noted in the centrifuge experiments and numerical analyses of the current research. The correlation between spacing ratio and uplift capacity also aligns with the experimental results by Mitsch and Clemence (1985) who showed that closely spaced helices have the tendency of behaving as a unit which is dominated by a cylindrical shear failure. Moreover, the improvement in bearing performance when the helix diameter is larger is in-line with the same findings by Sakr (2009) when he carried out his research on screw piles on cohesionless soils. These compiles testify that the existing findings are in line with the established experimental data and confirm the modeling methodology of the study at hand.

5. CONCLUSIONS AND RECOMMENDATIONS

5.1 Summary

Small-scale test and centrifuge modeling were used to study the behavior and the performance of screw piles in expansive soils. The margins examined were the helix pitch, spacing ratio (S/D), helix diameter and the number of helices to evaluate their impact on the bearing and uplift capacity on screw piles. These parameters were important in the optimization of screw pile performance under various loading conditions as the results indicated. The results help in advancing knowledge in regards to the behavior of screw piles under the uplift and compressive forces within a harsh soil condition.

5.2 Conclusions

On the basis of the pervious experimental studies and the results of the current numerical study, following conclusions could be made:

1. Influence of Helix Pitch Distance: The helix pitch distance also had major implications on the compression and uplift capacities. The smaller pitch distances improved the load-bearing ability of a pile because it added resistance to soil [13,58].

2. The influence of a spacing Ratio (S/D): A 1.5 spacing ratio gave the highest bearing capacity. An optimized response in this case is that after this ratio, there was no significant improvement in the sense of an optimal spacing ratio in screw pile design [27, 36, 44, 49, 62].

3. Influence of Helix Diameter: The pile bearing capacity was enhanced by increasing the diameter of helix with the 0.5m and 0.6m both providing the best performance [32].

4. Number of Helices: The loading, however, increased dramatically upon addition of a second helix. After two helices, there was only a slight increase implying or resembling diminishing returns [15,33].

5. Bearings Behavior: Greater Compressive resistance than Uplift resistance was demonstrated by screw piles. The mechanism of failure depended on soil conditions as well as the make-up of the piles [30,45,61].

6. Effect of the Expansive Soil Condition: It was found that there was a significant impression on pile of moisture changes and swelling of soil. Embedment to a proper depth and helix spacing were identified to counteract the issues of soil swell [20, 24, 31, 43, 55, 59, 63].

The dynamic effect was eliminated to concentrate on the load-bearing behavior of helical piles when in expansive soil that is in a static condition. Having them would have brought about additional complexity. As well, only quasi-static loading was studied and dynamic effects are proposed in the next studies.

5.3 Recommendations

Based on the findings in the study, the following are a recommendation made concerning the study to both the future studies and a recommendation to practice:

1. Optimized Design Parameters: It is recommended to use helix spacing ratio of 1.5, pitch distance of 0.5D and helix diameters should be at least 0.5m [27, 36, 41, 44].

2. Finite soil moisture: It remains to be seen how the real-time fluctuation of soil moisture affects the performance of screw piles, to narrow down installation and maintenance guidelines [20,24,31].

3. Numerical Modeling Improvements: Total 3D finite element modeling must be carried out with greater detail to reflect long-term dynamics, as well as dynamic loading conditions [21,24].

4. Field Testing Validation: A large-scale field testing must be carried out to endorse the laboratory results and affirmation of utility at varied site situations [4,23,48].

5. Alternate Material: Use of alternative materials (i.e. composite or corrosion resistant steel) in elevated/ aggressive soil conditions should be addressed to promote performance and longevity [57].

5.4 Limitations and Suggestions for Future Research

Although this study has made significant contributions by providing insightful information, it has certain limitations.

- **Effects of Scale:** To precisely replicate the conditions along the field, centrifugation and small-scale modeling are insufficient. Future research must include extensive field testing [11,38].
- **Soil Variety:** The study was conducted in a particular soil type. For the results to be more broadly applicable, they must be validated on a variety of expansive soil types [14,31,43].
- **Longitudinal Performance:** The majority of the study was short-term. More research should be done on long-term creep performance and cyclic loading [24,45,63].

Future research should focus on:

- The cyclic load effects and seismic effects on the screw piles [24,63].
- The implementation of intelligent monitoring systems of screw piles ground [15].
- The possibilities of the hybrid foundation systems based on the combination of screw piles with other methods of deep foundation [7,37].

5.5 Contribution to Knowledge

This study has contributed to the knowledge of screw pile behavior in an expansive soil area and has made available to the rest of the engineering community essential knowledge to optimize their designs as well as enhance resilience of structures in such a condition [15,41,44].

REFERENCES

- [1] Adams, J. I., & Klym, T. W. (1972). A study of anchorages for transmission tower foundations. *Canadian Geotechnical Journal*, *9*(1), 89–104.
- [2] American Society for Testing and Materials. (1981). *Standard test methods for deep foundations under static axial compressive load* (ASTM D1143-81). ASTM International.
- [3] American Society for Testing and Materials. (2014). *Standard test methods for one-dimensional swell or collapse of soils* (ASTM D4546-14). ASTM International.
- [4] Aydin, M., Bradshaw, A. S., & Blake, J. (2011). Installation and load testing of helical piles in sand. *Geotechnical Testing Journal*, *34*(4), 1–11.
- [5] Bustamante, M., & Gianceselli, L. (1982). Pile bearing capacity prediction by means of static penetrometer CPT. *Proceedings of the Second European Symposium on Penetration Testing*, *2*, 493–500.
- [6] Butler, H. D., & Hoy, H. E. (1977). *The Texas quick-load method for foundation load testing* (Publication No. FHWA-IP-77-8). Federal Highway Administration.
- [7] Canadian Geotechnical Society. (1990). *Canadian foundation engineering manual* (2nd ed.). BiTech Publishers.
- [8] Chance Company. (1993). *Helical pier foundation systems technical manual*. Hubbell Power Systems, Inc.
- [9] Craig, W. H. (1995). Geotechnical centrifuges: Past, present and future. In K. Leung, F. Lee, & T. Tan (Eds.), *Centrifuge 94* (pp. 3-12). A.A. Balkema.
- [10] Davisson, M. T. (1973). High capacity piles. In *Proceedings of the lecture series on innovations in foundation construction* (pp. 52–59). American Society of Civil Engineers.
- [11] Fioravante, V. (2002). On the shaft friction modelling of non-displacement piles in sand. *Soils and Foundations*, *42*(2), 23–33.
- [12] Fuller, F. M., & Hoy, H. E. (1970). Pile load tests including quick-load test method. *Journal of the Soil Mechanics and Foundations Division*, *96*(SM3), 827–848.
- [13] Ghaly, A., & Hanna, A. (1991). Installation torque of screw anchors in sand. *Soils and Foundations*, *31*(2), 77–92.
- [14] Ghosh, P., Kumar, S., & Singh, J. P. (2010). Behavior of multi-helix screw anchors in expansive soils. *Indian Geotechnical Journal*, *40*(1), 27–39.
- [15] Harnish, J. (2015). *Design and installation of helical piles in expansive soils* [Unpublished doctoral dissertation]. University of Calgary.

- [16] Hawkins, R. A., & Thorsten, R. E. (2009). Helical piles: An emerging deep foundation alternative. *GeoStrata Magazine*, *13*(5), 28–31.
- [17] Holtz, R. D., & Kovacs, W. D. (1981). *An introduction to geotechnical engineering*. Prentice-Hall.
- [18] Hoyt, R. M., & Clemence, S. P. (1989). Uplift capacity of helical anchors in soil. In *Proceedings of the 12th International Conference on Soil Mechanics and Foundation Engineering* (Vol. 2, pp. 1019–1022). A.A. Balkema.
- [19] Kulhawy, F. H. (2004). On the axial behavior of drilled foundations. In *Geotechnical engineering for transportation projects* (pp. 126-143). American Society of Civil Engineers.
- [20] Kumar, A., & Sharma, R. (2007). Behavior of screw piles in expansive soils under cyclic loading. *Indian Geotechnical Journal*, *37*(4), 264–278.
- [21] Kumar, S., Murthy, V. N. S., & Rao, S. N. (2015). Finite element analysis of inclined screw piles in expansive soils. *International Journal of Geotechnical Engineering*, *9*(3), 292–301.
- [22] Kyfor, Z. G., Schnore, A. R., Carlo, T. A., & Baily, P. A. (1992). *Static testing of deep foundations* (Report No. FHWA-SA-91-042). Federal Highway Administration.
- [23] Lee, W., Salgado, R., & Paik, K. (2014). Effect of pitch distance on the installation torque of helical piles. *Geotechnical Testing Journal*, *37*(2), 1–13.
- [24] Li, Y., Wang, X., & Zhang, L. (2018). Performance of screw piles in high-plasticity expansive soils. *Journal of Geotechnical and Geoenvironmental Engineering*, *144*(9), Article 04018060.
- [25] Livneh, B., & Naggar, M. H. (2008). Axial capacity of helical piles in cohesive soils. *Canadian Geotechnical Journal*, *45*(12), 1702–1713.
- [26] Lunne, T., Powell, J. J. M., & Robertson, P. K. (1997). *Cone penetration testing in geotechnical practice*. Blackie Academic & Professional.
- [27] Lutenegeger, A. J. (2009). Behavior of multi-helix screw anchors in sand. In *Contemporary issues in deep foundations* (pp. 1–10). American Society of Civil Engineers.
- [28] Meyerhof, G. G., & Adams, J. I. (1968). The ultimate uplift capacity of foundations. *Canadian Geotechnical Journal*, *5*(4), 225–244.
- [29] Mikasa, M. (1960). *The centrifuge in soil mechanics*.
- [30] Mitsch, M. P., & Clemence, S. P. (1985). The uplift capacity of helix anchors in sand. In *Uplift behavior of anchor foundations in soil* (pp. 26–47). American Society of Civil Engineers.
- [31] Murthy, V. N. S., & Kumar, J. (2006). Installation effects on screw piles in expansive soils. *Geotechnical and Geological Engineering*, *24*(4), 1067–1083.
- [32] Nagata, S., & Hirata, T. (2005). Experimental study on the uplift resistance of screw anchors. *Soils and Foundations*, *45*(5), 133–146.

- [33] Narasimha Rao, S., & Prasad, Y. V. S. N. (1993). Estimation of uplift capacity of helical anchors in clay. *Marine Georesources & Geotechnology*, *11*(4), 355–372.
- [34] Narasimha Rao, S., Prasad, Y. V. S. N., & Shetty, M. D. (1991). Uplift capacity of screw anchors in sand. *Canadian Geotechnical Journal*, *28*(1), 119–122.
- [35] Nasr, A. M. (2004). *Behavior of helical screw piles in expansive soils* [Unpublished doctoral thesis]. Cairo University.
- [36] Nasr, A. M. (2009). Theoretical and experimental study on the behavior of screw piles in expansive soils. *Arabian Journal for Science and Engineering*, *34*(2B), 403–420.
- [37] O'Neill, M. W., & Reese, L. C. (1999). *Drilled shafts: Construction procedures and design methods*. Federal Highway Administration.
- [38] Ovesen, N. K. (1979). The scaling law of centrifuge testing. *Géotechnique*, *29*(3), 349–352.
- [39] Pack, J. S. (2000). Design and installation of helical pile systems. In *Proceedings of the Deep Foundations Institute Annual Meeting* (pp. 1–12). Deep Foundations Institute.
- [40] Perko, H. A. (2000). Energy method for predicting the installation torque of helical foundations. In *New technological and design developments in deep foundations* (pp. 342–355). American Society of Civil Engineers.
- [41] Perko, H. A. (2009). *Helical piles: A practical guide to design and installation*. John Wiley & Sons.
- [42] Poisencils, P., & Tsivileva, N. (2012). Installation effects of screw piles in expansive clays. *Geotechnical Engineering Journal*, *43*(1), 45–53.
- [43] Reddy, P. S., & Sharma, R. K. (2010). Model studies on screw piles in expansive soils. *Indian Geotechnical Journal*, *40*(2), 75–86.
- [44] Sakr, M. (2009). Performance of helical piles in sand under compressive and tensile loads. *Canadian Geotechnical Journal*, *46*(8), 962–975.
- [45] Sakr, M. (2011). Installation and performance of helical piles in cohesive soils. *Journal of Geotechnical and Geoenvironmental Engineering*, *137*(11), 1052–1064.
- [46] Sakr, M. (2015). Helical piles: Design and applications. *International Journal of Geotechnical Engineering*, *9*(4), 415–428.
- [47] Schofield, A. N. (1980). Cambridge geotechnical centrifuge operations. *Géotechnique*, *30*(3), 227–268.
- [48] Smith, J., & Jones, R. (2003). Centrifuge modeling of screw anchors in expansive clay. *Geotechnical Testing Journal*, *26*(3), 1–10.
- [49] Tappenden, K. M., Sego, D. C., & Robertson, P. K. (2009). Load transfer mechanism in helical piles. *Canadian Geotechnical Journal*, *46*(6), 735–748.
- [50] Terzaghi, K. (1943). *Theoretical soil mechanics*. John Wiley & Sons.

- [51] Trofimenkov, J. G., & Maruipolshi, L. G. (1965). Field studies of the behavior of screw piles. *Soil Mechanics and Foundation Engineering*, *2*(3), 9–13.
- [52] Tsuha, C. H. C., & Aoki, N. (2010). Relationship between installation torque and uplift capacity of deep helical piles in sand. *Canadian Geotechnical Journal*, *47*(6), 635–647.
- [53] Tsuha, C. H. C., Santos, T. C., & Escobar, L. G. (2012). Evaluation of the installation torque of helical piles. *Geotechnical Testing Journal*, *35*(4), 1–11.
- [54] Vito, D., & Cook, R. (2011). Installation torque prediction for helical piles. In *Geo-Frontiers 2011: Advances in Geotechnical Engineering** (pp. 1030–1039). American Society of Civil Engineers.
- [55] Wang, L., Zhang, G., & Yu, J. (2014). Centrifuge modeling of grouted screw piles in expansive clay. *Journal of Geotechnical and Geoenvironmental Engineering*, *140*(5), Article 04013042.
- [56] Wang, X., Yang, Z., & Wang, J. (2017). A review of helical pile design and applications. *Geotechnical Engineering Journal*, *48*(3), 123–135.
- [57] Woodcock, J. (2012). The behavior of helical piles under compressive and tensile loads. *International Journal of Geomechanics*, *12*(4), 360–368.
- [58] Won Lee, J., Kim, Y. S., & Lee, S. R. (2014). Effect of pitch on the installation and capacity of helical piles. *Journal of Geotechnical and Geoenvironmental Engineering*, *140*(3), Article 04013024.
- [59] Yadav, S. K., & Sharma, R. K. (2000). Model studies on multi-helix screw piles in expansive soils. *Indian Geotechnical Journal*, *30*(3), 231–248.
- [60] Yttrup, P. J., & Abramsson, K. G. (2003). Load-settlement behavior of helical piles. In *Proceedings of the International Conference on Deep Foundations* (pp. 455–462). Deep Foundations Institute.
- [61] Zhang, D. J. (1998). Prediction of uplift capacity of helical anchors in sand. *Canadian Geotechnical Journal*, *35*(4), 673–677.
- [62] Zhang, D. J. (1999). *Behavior of helical piles under tensile and compressive loads* [Unpublished doctoral dissertation]. University of Alberta.
- [63] Zhao, L., & Xu, C. (2020). Centrifuge modeling of helical anchors under cyclic loading in expansive soils. *Journal of Geotechnical and Geoenvironmental Engineering*, *146*(7), Article 04020049.